

LA--980

Copy [REDACTED]

[REDACTED]

c 3

CIC-14 REFERENCE COLLECTION  
SERIALIZED BY [REDACTED]

CONF

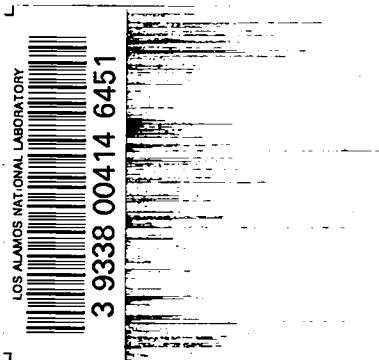
# LOS ALAMOS SCIENTIFIC LABORATORY

OF THE

UNIVERSITY OF CALIFORNIA

CONTRACT W-7405-ENG. 36 WITH

U. S. ATOMIC ENERGY COMMISSION





CIC-14 REPORT COLLECTION  
REPRODUCTION  
COPY

LA-980

[REDACTED]

[REDACTED] 27 [REDACTED]

November 16, 1949

This document contains 89 pages

DIFFERENTIAL CROSS SECTION AS A FUNCTION OF ANGLE FOR THE  
D(d,p)T REACTION FOR 10.9 MEV BOMBARDING DEUTERONS

By

Kenneth Warne Erickson

Submitted to the faculty of the University of Texas in partial fulfillment of the requirements for the Degree of Doctor of Philosophy.

Physics General





## TABLE OF CONTENTS

CHAPTER	Page
I. Introduction_____	1
II. Apparatus and Apparatus Checks	
A. Angular Data_____	5
B. Zero Degree Data_____	24
III. Procedure	
A. Angular Data_____	31
B. Zero Degree Data_____	34
IV. Data Analysis_____	38
APPENDIXES	
A. Derivation of Equation for Calculating Cross Section____	50
B. Transformation relations between Lab and Center of Mass Systems_____	57
C. Relative Stopping Power of Nylon_____	61
D. Results	
I. Intermediate Results_____	62
2. Final Results_____	66
BIBLIOGRAPHY_____	67



CHAPTER I  
INTRODUCTION

The two competing reactions



were first noted in 1934 in a paper by Oliphant, Harteck, and Rutherford.<sup>1)</sup> Later workers<sup>2-8)</sup> have shown that both the total cross section and the differential cross section (i.e., cross section per unit solid angle) of the two reactions are quite similar up to bombarding energies of about four Mev; and that, up to these energies the angular distribution of the reaction particles

- 
- 1) Oliphant, Harteck, and Rutherford, Proc. Roy. Soc. A144, 692 (1934).
  - 2) Kempton, Browne, and Maasdorp, Proc. Roy. Soc. A157, 386 (1936).
  - 3) R. B. Roberts, Phys. Rev. 51, 810 (1937).
  - 4) R. Ledenburg and M. H. Kanner, Phys. Rev. 52, 911 (1937).
  - 5) Coon, Davis, Graves, Graves, and Manley, LADC-56 (1944) (declassified).
  - 6) Coon, Davis, Graves, and Manley, LADC-75 (1944) (declassified).
  - 7) Blair, Freier, Lampi, Sleator, and Williams, Phys. Rev. 74, 1599 (1948).
  - 8) G. T. Hunter and H. T. Richards, Bull. Amer. Phys. Soc. 23, No. 7, 14 (1948).

from both (1) and (2) follows fairly closely a law of the form

$$N(\theta) = 1 + A(E) \cos^2\theta + B(E) \cos^4\theta \dots\dots\dots (3)$$

where  $\theta$  is in the center of mass system and  $A(E)$  and  $B(E)$  are constants for constant energies. In fact, the coefficients of the  $\cos^2\theta$  and  $\cos^4\theta$  terms as calculated by the Minnesota group<sup>7)</sup> are very nearly the same for both reactions. A study of the  $D(d,n)He^3$  reaction at 10.3 Mev has been made at Los Alamos.<sup>13)</sup>

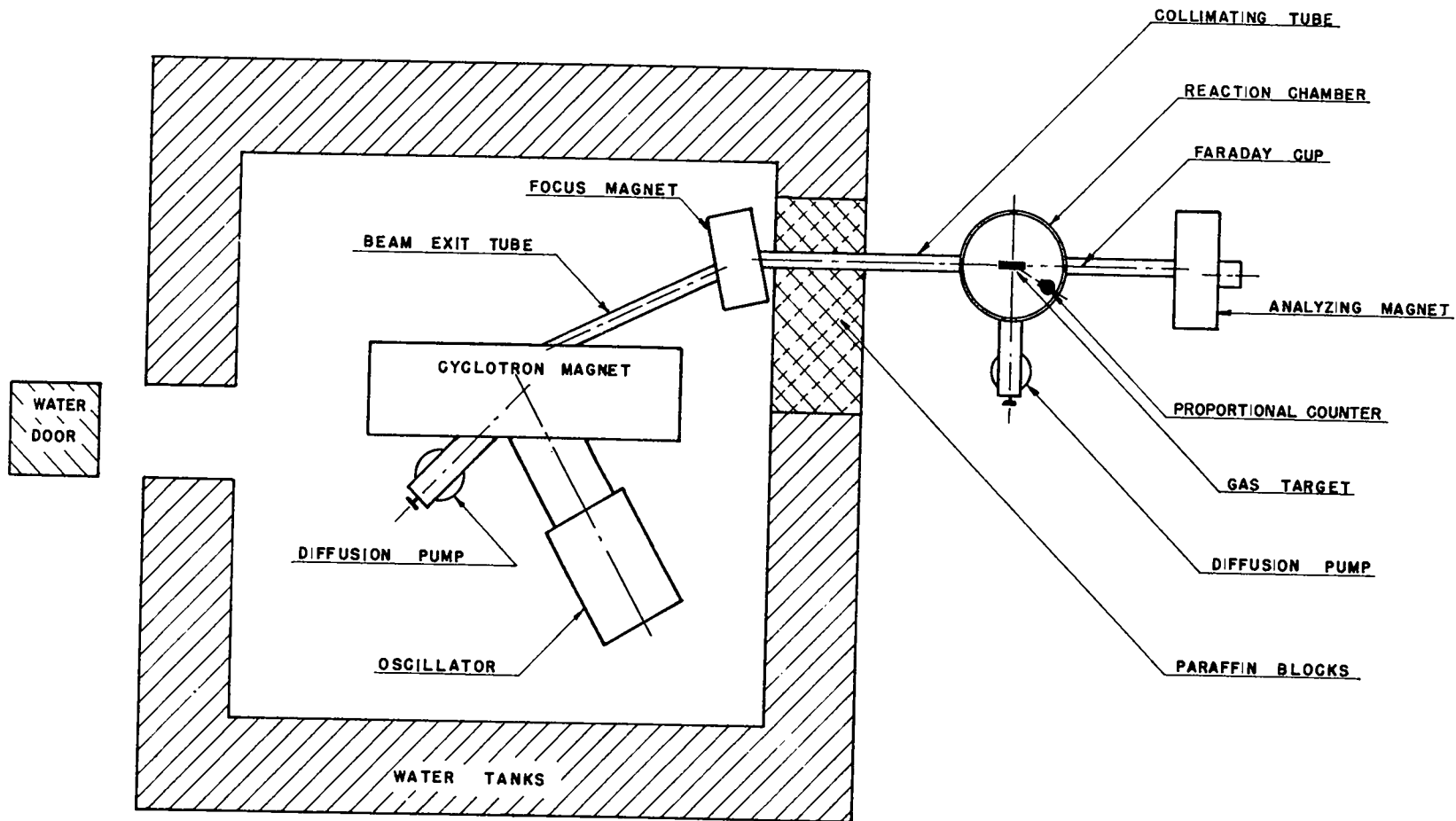
An analysis of the differential cross section from this study indicates that terms up to  $\cos^8\theta$  have to be included to fit the experimental data. Leiter and others at Illinois<sup>14,15)</sup> have measured the differential cross section of reaction (1) at ten Mev and have obtained a fit by including terms up to  $\cos^{10}\theta$ .

The general outline of the present experiment is as follows: A thin deuterium gas target was bombarded with 11 Mev deuterons from the 42 in. Los Alamos cyclotron (see Fig.1.) Reaction protons

- 
- 9) Huntoon, Ellett, Bayley, and Van Allen, Phys. Rev. 58, 97 (1940).
  - 10) Manning, Huntoon, Myers, and Young, Phys. Rev. 61, 371 (1941).
  - 11) Bennet, Mandeville, and Richards, Phys. Rev. 69, 418 (1946).
  - 12) Bretscher, French, and Seidl, Phys. Rev. 73, 815 (1948).
  - 13) Erickson, Fowler, and Stovall, Phys. Rev. (to be published 1949).
  - 14) Leiter, Meagher, Rodgers, and Kruger, Bull. Amer. Phys. Soc. 24, No. 4, 12 (1949).
  - 15) P. G. Kruger, private communication.

Figure 1

Arrangement of Los Alamos cyclotron and reaction chamber.



emitted from this target chamber by virtue of the  $D(d,p)T$  reaction were counted by means of a proportional counter placed at various angles to the beam. The main beam continued through the target into a Faraday cage by means of which the total number of deuterium particles bombarding the target was obtained. These data, together with the geometry of the secondary particle system, permitted the calculation of the desired differential cross section.

CHAPTER II  
APPARATUS AND APPARATUS CHECKS

A. ANGULAR DATA.

As mentioned above, the Los Alamos 42 in. cyclotron was used as a source of deuterons for the experiment. This cyclotron produced a focused beam of deuterons in the reaction chamber which was located approximately 15 feet from the cyclotron magnet. The beam was defined to  $\pm 1.1^\circ$  by two beam-defining slits located approximately five feet apart in the tube between the focus magnet and the reaction chamber. A gold beam-defining diaphragm with a 3/16 in. hole located on the front end of the gas target chamber further defined this beam to  $\pm 0.6^\circ$ . Two anti-scattering slits, one located one foot in front of the target and the other in the target chamber itself prevented deuterons which were scattered by the walls of the tube and the target chamber from entering the counter. Twice, during the three and one-half months course of the experiment, the position and spread of the beam were measured. These measurements were made by moving the proportional counter (adjusted to act as an ionization chamber) to various positions in the path of the beam and recording the relative ionization at these points. This method required that the cyclotron beam intensity remain fairly constant while the various points were being taken which, in turn, demanded that a minimum of cyclotron operating time elapse during a run. The data were therefore

taken by recording both the counter position and the relative ionization on General Electric Recording Micro-ammeters and later analyzing the tapes to obtain the beam distribution curves. Figure 2 shows one of the curves so taken.

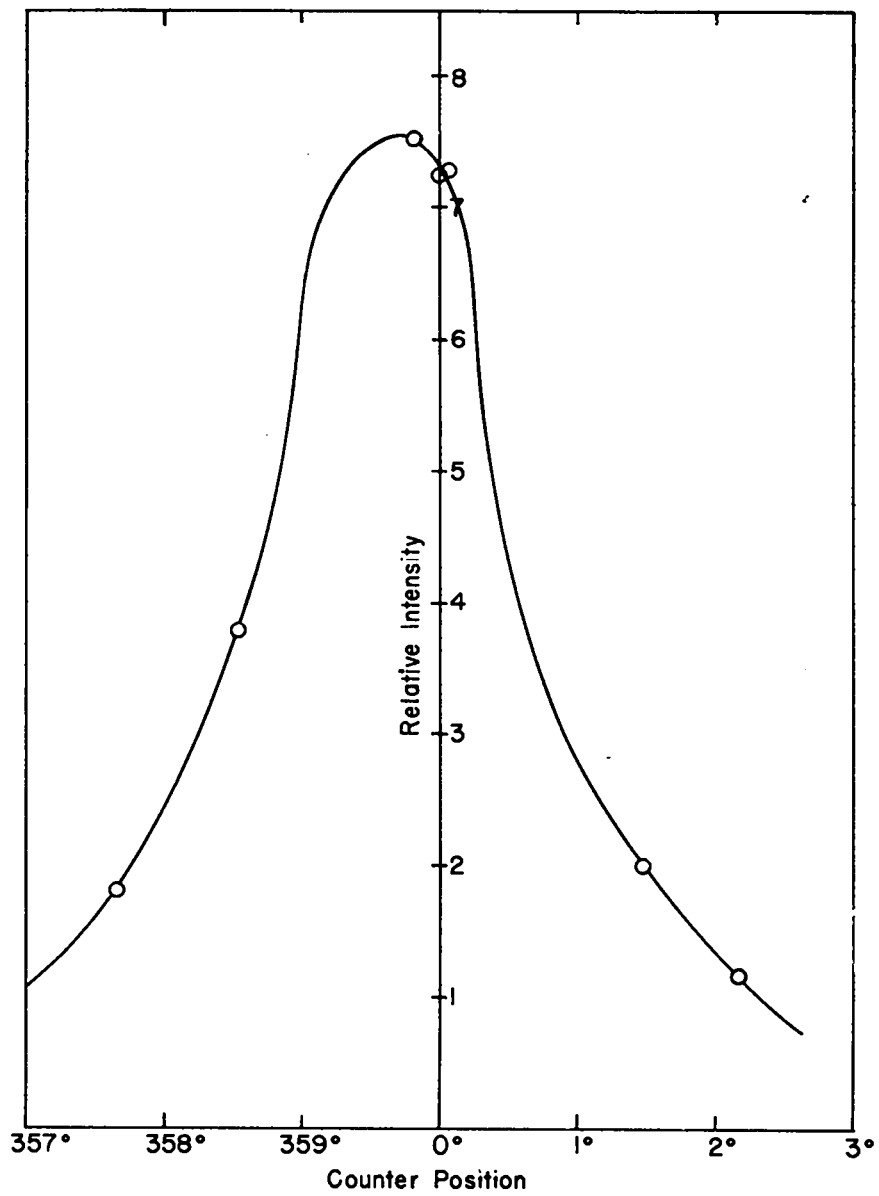
In both of these measurements, the beam passed through the target before it reached the counter, so that scattering due to the entrance and exit nylon windows in the target chamber contributed to the measured spread. At one time during the course of a previous experiment,<sup>13)</sup> the beam distribution measurements were made with no target windows in the beam path. In all three of these measurements, the beam spread was approximately that to be expected from a consideration of the geometry of the slit system and Rutherford scattering from the window material (see Table I.) The position of the beam relative to the counter angular scale was the most important result obtained from these measurements since this value entered directly into calculations of the differential cross section curve.

The energy of the cyclotron beam was measured at frequent intervals during the course of the experiment (24 times total.) The method used (magnetic deflection of the beam) had been checked prior to the start of this experiment<sup>16)</sup> by determining, by means of aluminum and air stopping elements, the air equivalent path of the beam. Repeated measurements of this energy, during any one day, were consistent to better than  $\pm 1.0$  percent, and it was estimated

---

16) Curtis, Fowler, and Rosen, Rev. Sci. Inst. 20, 388 (1949).

Figure 2  
Beam Distribution Curve.



Conditions	Trial No.	Beam Position	Beam Spread at Half Maximum	
			Experimental	Calculated*
1/4" diaphragm hole, 1/8" counter hole, no windows	1	359.5°	2.1°	~ 2°
3/16" diaphragm hole, 1/8" counter hole,  2.7 $\frac{\text{mg}}{\text{cm}^2}$ mica window + 4.5 $\frac{\text{mg}}{\text{cm}^2}$ nylon	1	359.5	1.9°	~ 2° $\frac{1}{2}$
	2	359.6	1.9°	~ 2° $\frac{1}{2}$
3/16" diaphragm, 1/4" counter hole,  2 - 6.9 $\frac{\text{mg}}{\text{cm}^2}$ nylon windows	1	359.9	2.5°	~ 3°
	2	359.3	2.4°	
	3	359.5	2.5°	
	4	359.6	2.2°	

\* The calculations used here were very rough and it is considered mainly fortuitous that the Experimental and Calculated values agree as well as they do.

Table I. Results of beam distribution tests.

that the absolute value was correct to within  $\pm 2.0$  percent. During the course of the experiment, the value obtained for the cyclotron beam energy varied from 10.78 Mev to 11.02 Mev. This was a gradual shift over a period of about three months and was believed to be a real shift.

Figures 3 and 4 are two views of the apparatus in the two foot diameter reaction chamber as used to take the angular points (i.e., points other than the zero degree point.) Figure 5 is a schematic view of the target and secondary slit system arrangement. The gas target chamber is located on an adjustable target support in the center of the chamber. The deuteron beam enters through the 1-1/4 in. hole at the upper right of the photographs. This hole is actually one of the above mentioned anti-scattering diaphragms. The proportional counter, covered with a 1/2 in. lead shield to cut down the gamma background, is shown at the upper left. The inner slit of the secondary slit system is mounted between the counter and the target chamber on the rotating arm of the proportional counter. The Faraday cage (not shown) is mounted in the large tube at the lower left. A sectional view of the target chamber is shown in Figure 6. Its overall length, excluding the gold beam-defining slit at the left, is 7.0 inches. The center hole is 9/16 in. diameter, and the side ports are 9/16 in. high by 3-1/2 in. long. The hole in the beam-defining diaphragm is 3/16 in. diameter, and that in the anti-scattering diaphragm (shown just to the left of the side windows) is slightly more than 1/4 in. diameter. The window material used

Figure 3  
Reaction chamber as used for angular points.



Figure 4  
Reaction chamber as used for angular points.



Figure 5

Schematic of reaction particle system.

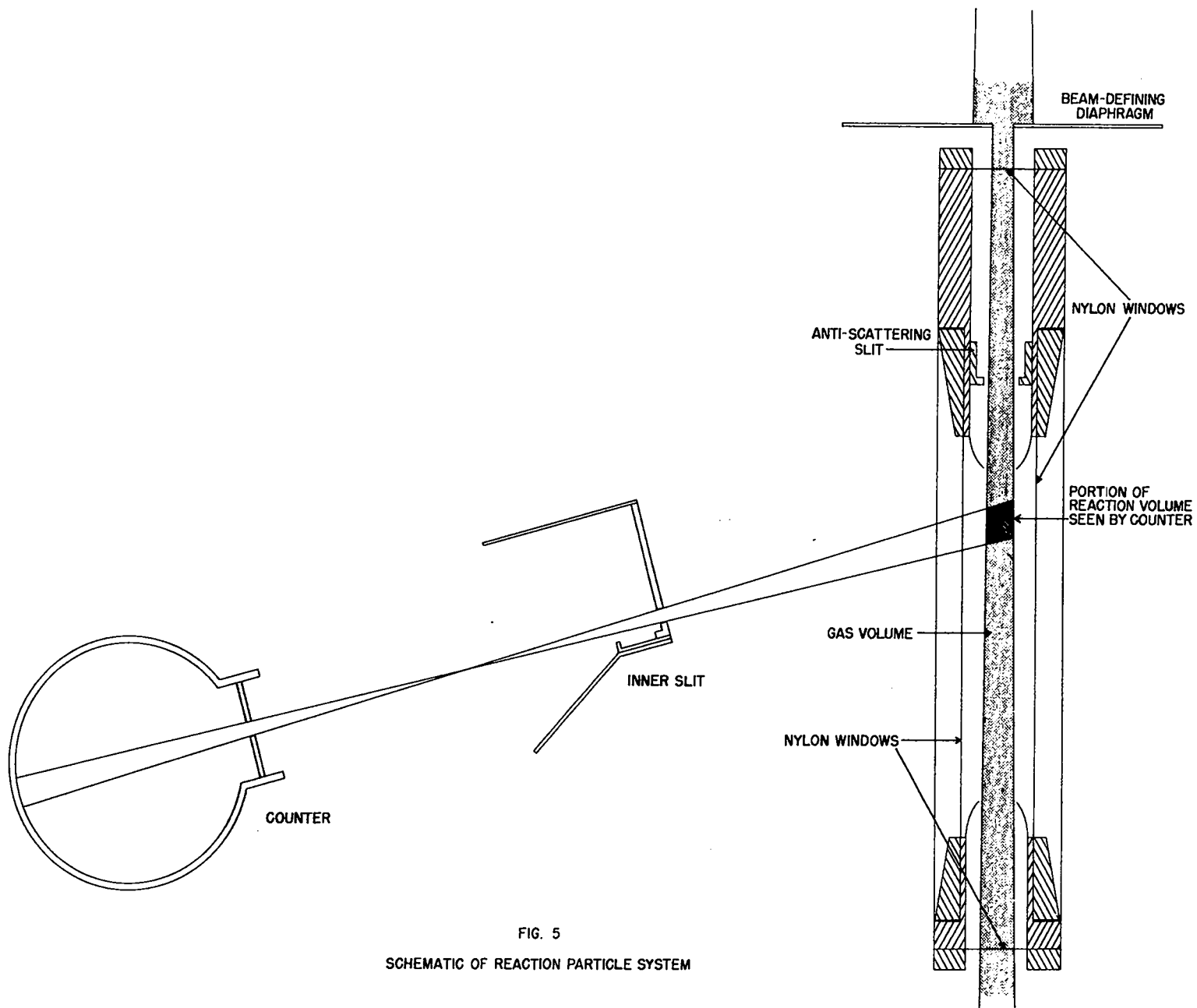
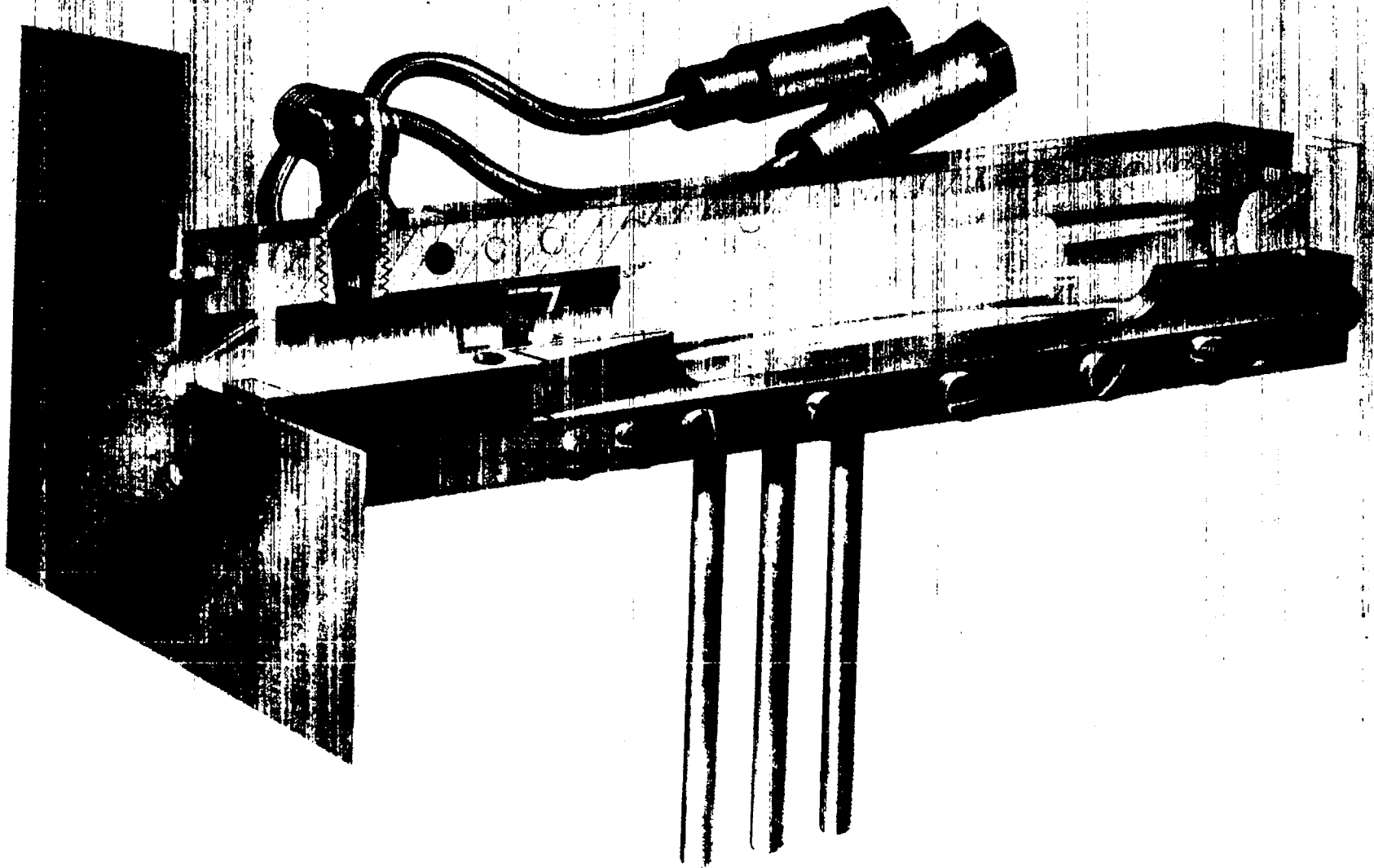


FIG. 5  
 SCHEMATIC OF REACTION PARTICLE SYSTEM

Figure 6  
Gas target chamber used for angular points.



was nylon foil of thicknesses varying from 2.6 to 6.9 mg/cm<sup>2</sup>. The photograph also shows the water cooling tubes, the gas filling connection, and the three mounting pins.

The target chamber was actually designed for use in the present equipment; however, prior to its use here, it was used in the D-D elastic scattering experiment<sup>17)</sup>; and therefore, from this latter experiment come most of the checks on the reliability of the target.

One of the most serious troubles to be guarded against in a target was that of possible scattering of particles from the walls of the target into the counter. During the course of the D-D scattering experiment, the thickness of the target window material and gas pressure in the target were each varied by factors of more than two to one without changing the results obtained. Also, the cross sections obtained using this target were the same as those obtained using other targets of a different type<sup>16)</sup> which also had been tested in this same way (i.e., varying of various parameters.) Were the above difficulty present in this target, it would undoubtedly have shown up as different cross section values for different target pressures and nylon window thicknesses, especially in the entrance window of the target chamber. Besides, since it would certainly be expected that spuriously scattered particles would not give the same effect at all angular points, the fact that the points in both the D-D scattering cross section and the differential cross section of the

---

17) Allred, Erickson, Fowler, and Stovall, Phys. Rev. (to be published 1949).

present reaction were symmetrical, about  $90^\circ$  center of mass, to better than three percent indicates that spurious scattering did not introduce any very serious errors.

Another danger to be anticipated from a target chamber was that the back end may block part of the deuteron beam from the Faraday cage after the beam has passed through the target volume. This, of course, would give too low a value for the beam current and hence too high a value for the cross section. The tolerances on the wide angle target were made quite close ( $\pm 1.5^\circ$ ); however, calculations on the basis of Rutherford scattering formula indicated that the losses would be about  $\pm 0.5$  percent. Also, as mentioned above, the data from this target chamber compared very well with that from other target chambers where the tolerances were not so close (e.g., one chamber used for comparison permitted a  $\pm 3.5^\circ$  spread of the beam.) Also, were this difficulty present, the results would be expected to depend critically on the alignment of the target with relation to the beam; this fact was not found to be true during the experiment.

The various tests, in which the back target window was varied with no corresponding change in calculated cross section values, also indicated that scattering due to this window was not sufficient to cause an appreciable part of the beam to miss the Faraday cage. The above mentioned beam-position measurements further bore this out.

The target chamber was filled with commercially purified deuterium gas whose label claimed less than 0.5 percent impurities. However, a mass spectrographic analysis indicated that this impurity

was of the order of one percent. During the first part of the experiment the gas target was filled through a palladium valve so that all impurity except hydrogen was eliminated. However, during the latter part of the experiment (i.e., the part using 1/4 in. counter hole) the palladium valve was broken and the gas target was filled directly from the deuterium tanks. As will be discussed later, this impurity necessitated a 5.8 percent correction to the cross section at certain angles in the back quadrant.

The secondary slit system consisted of an adjustable vertical slit mounted on the rotating arm of the proportional counter (see Figs. 3, 4, and 5) and a circular diaphragm mounted directly in front of the counter window. The slit width was set at 1/8 in. The counter window was 1/8 in. diameter for part of the experiment and 1/4 in. diameter for the rest. Secondary scattering of the reaction particles was kept at a minimum by allowing as little material as possible to be in a position near the secondary beam. In those places where it was necessary to have material near the secondary beam (such as the inner slit holder), anti-scattering baffles were provided so that in no case was it possible for secondary particles to scatter to the counter window from wide expanses of metal. Gold shields were fastened to the sides of the internal slit mount (see Figs. 4 and 5) to prevent particles being scattered directly into the counter window by the main beam anti-scattering diaphragm (the hole at the upper right of Fig. 4) or by the nylon entrance and exit windows.

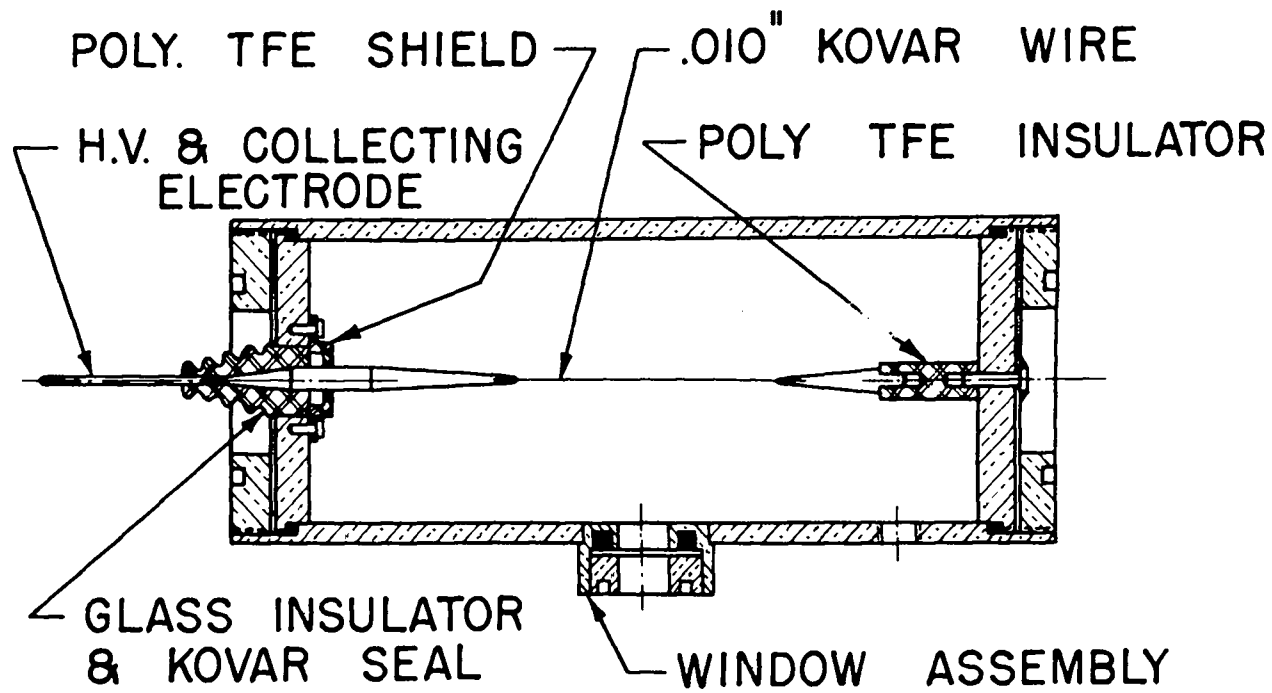
The counter used to detect the protons, which were emitted at various angles, was of the conventional cylindrical design with an axial collecting wire and a thin foil window in the side for particle entrance<sup>16)</sup> (see Fig. 7.) The cylinder was two inches in diameter by six inches long. The 5.0 mil Kovar axial wire was offset 1/4 in. so as not to block the path of the particles being counted. The side window, located midway between the two ends, was of 1/8 or 1/4 in. diameter (at different times during the experiment) and was covered with either 1.1 mg/cm<sup>2</sup> mica or 2.7 mg/cm<sup>2</sup> aluminum.

The counter was operated in the region where the voltage output was proportional to the ionization but with high enough E/p ratio to give gas multiplication. The gas multiplication curves for the counter used in this experiment are reproduced in Fig. 8. These curves were obtained by varying the voltage on the collecting wire while the counter was detecting alpha particles from a plutonium foil. The pulse height was observed on a cathode ray oscilloscope.

During the experiment the counter was operated with as high as 4000 volts and 52 #/in.<sup>2</sup> pressure. While these values were well above those covered by the gas multiplication curves, the reproducibility of individual points at both low and high pressures and voltages indicated that no essential change in operating conditions of the counter resulted from this pressure-voltage increase.

An attempt was made to hold a gas multiplication value of ten

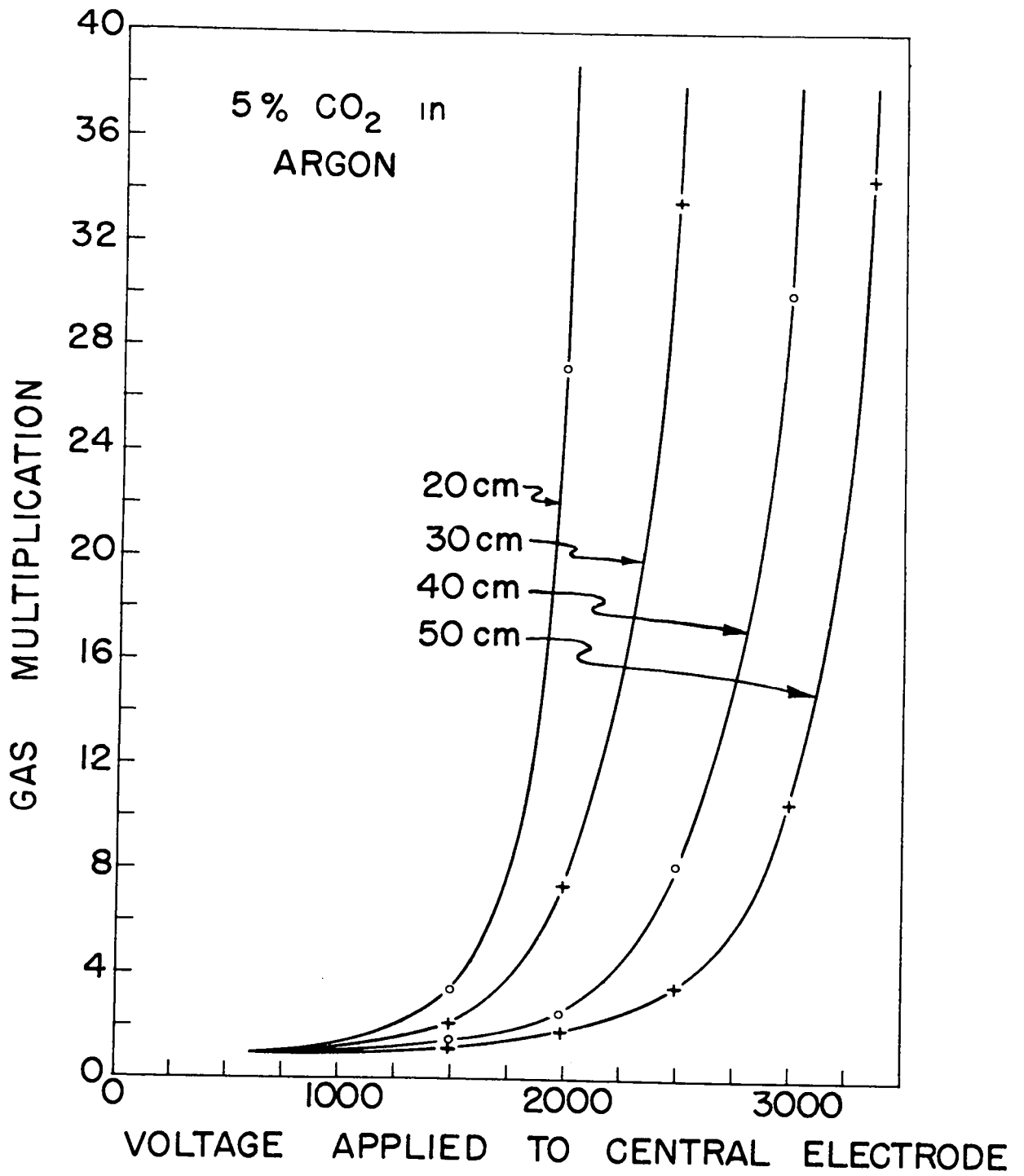
Figure 7  
Cross-sectional view of proportional counter.



SCALE



Figure 8  
Gas multiplication curves for proportional counter.



throughout the experiment. This value was chosen arbitrarily as being high enough to put the pulses well above amplifier noise and yet not high enough to cause the multiplication to vary unduly with small fluctuations of the stabilized power supply voltage. Pulses from the counter were fed through a preamplifier and amplifier and into a ten channel pulse amplitude analyzer.<sup>18)</sup> This analyzer served the purpose of separating the various pulses coming out of the amplifier into groups according to the height of the pulse and then routing pulses of a certain height into a certain mechanical counter. Thus, for certain switch settings, pulses of more than 7.5 volts height but less than 9.5 volts were counted by a mechanical counter labeled "Channel I." Pulses of 9.5 volts but less than 11.5 volts were counted in "Channel II", and so on. The top channel labeled "Surplus" was arranged to count all pulses of greater than a certain amount; namely, the upper limit of the "Channel IX." A "Total" channel recorded all pulses coming into the machine above the minimum of "Channel I" and served as a check on the operation of the instrument as a whole. The operation of the entire counter system was tested prior to the beginning of data-taking on the experiment of  $D(d,n)He^3$  by using alpha particles emitted from plutonium. By comparing the pulse height of the  $He^3$  particles from reaction (2) with that of  $\alpha$ -particles from the plutonium, it was made certain that the particles being counted were of charge two. Then later, with

---

18) E. W. Dexter, LAMS-573 (1947) (declassified).

the scattered deuteron and  $D(d,p)T$  experiments the pulse height was compared with that of the  $He^3$  particles and of the plutonium alphas and found to be of charge one. There was, however, another perfectly good check on the fact that the proper particles were being counted in each of these experiments. Since the range of these particles was accurately calculable for various angles of emission from the target by the method of Appendix B, and since at all angles the range of the particles turned out to be very close to that calculated, it was quite certain that the particles counted were those that it was desired to count.

The Faraday cage used for current measurements was located behind the target chamber and was simply a 2-1/4 x 9 in. brass tube closed at the back and connected through insulating material to the outside of the vacuum system. A magnetic field, produced in the Faraday cage by two permanent magnets lying along the cup outside the vacuum system, prevented recoil and secondary electrons produced at the back of the cage from escaping out the front. A negative 300 volts on the cage prevented electrons produced in the target windows, etc. from entering. The current integrator connected to this Faraday cage was designed so that when the cage was charged to a certain potential by the deuterons, a multivibrator circuit discharged it and registered a count on a mechanical counter. Thus, the total number of coulombs entering the Faraday cage and hence the number of deuterons passing through the target could be found.

About three times during each day of operation the calibration of the current integrator was checked (see Chapter III - A.) The day-to-day reproducibility of this calibration at high counting rates (128 counts/min) was better than  $\pm 0.5$  percent while at lower rates (50 counts/min) the reproducibility was about  $\pm 1.0$  percent. The difference between the high and low counting rate accuracy was probably due to temperature and humidity effects on leakage.

A test of leakage caused by the beam -- which would not be measured by the above calibration -- was made by blocking the beam from the Faraday cage and measuring the leakage current with the beam on and off; the difference between these two measurements being due to the beam alone. This effect was of the order of 0.2 percent on an average 2.5 minute run.

In conjunction with the study of the  $D(d,n)He^3$  experiment, the combined accuracy of current and energy measurements was tested. This was done by measuring the heating effect that the beam of deuterons produced in a copper block and comparing the total energy thus obtained with the value obtained by normal beam energy and Faraday cage data. The beam was monitored with the  $He^3$  particles from the  $D(d,n)He^3$  reactions. The temperature of the copper block was measured by means of an Alumel-Chromel thermocouple and an L & N type-K potentiometer. The results of this experiment are given in Table II. A conservative estimate of the accuracy of the combined energy and current measurement was  $\pm 3.0$  percent. As was mentioned above, the energy measurement was believed to be correct

to within  $\pm 2.0$  percent. Thus the accuracy of the current integrator measurement was probably better than 2.5 percent.

TRIAL NUMBER	TOTAL ENERGY - JOULES		ENERGY RATIO
	THERMAL METHOD	STANDARD METHOD	
I	131.0	129.7	0.990
II	198.2	209.7	1.058
			Av = 1.024
			= 2.4%

TABLE II

The above tests would also show up the presence of particles whose total charge to mass ratio differed from that of the deuterium ions (such as deuterium atoms formed after the focus magnet.) This says nothing about the presence of  $\text{He}^{++}$  but the possibility of this ion being in the cyclotron at all was very small and the further possibility of its ending up part of the beam was even less.

In order that the proton counts be separated on the 10 channel analyzer as much as possible from the spurious background counts, it was important that the end of the proton range lie just in the counter. In this way, the pulse of the real counts was higher and therefore was recorded in a higher channel than most of the background pulses. At all but a few back angles ( $> 100^\circ$  Lab.), the protons had more than enough energy and would, if left alone, have gone well

beyond the active range of the counter. It was therefore necessary, at almost all angles to insert energy absorbers in the secondary particle path. To attain this end, a Selsyn controlled foil system<sup>19)</sup> was mounted on the reaction chamber lid (see Fig. 9) so that two coaxial foil wheels, each with ten holes, were located between the two defining slits of the secondary beam. This made possible a selection of one hundred absorbers and allowed adjustments in steps of one cm air equivalent up to 56 cm, and five cm steps from 56 cm to 330 cm.

The target pressure was read on a mercury manometer. The readings were believed to be good to  $\pm 0.3$  mm which amounts to  $\pm 0.1$  percent at the lowest pressure used. The target temperature was obtained by reading the temperature of the output cooling water. The readings were certainly good to  $\pm 0.3^\circ\text{F}$  which is about  $\pm 0.5$  percent maximum error.

#### B. ZERO DEGREE DATA

Although the method of taking the data was essentially the same for the zero degree point as for the angular points, it was necessary to design a certain amount of additional apparatus to be used here. Figures 10 and 11 show respectively the target and the auxiliary Faraday cage. Figure 12 shows these two items as located in the reaction chamber. The target was made relatively short in

---

19) This foil wheel system, designed by J. L. Fowler of Los Alamos, has not been described in the literature.

Figure 9  
Selsyn-controlled foil wheel system.

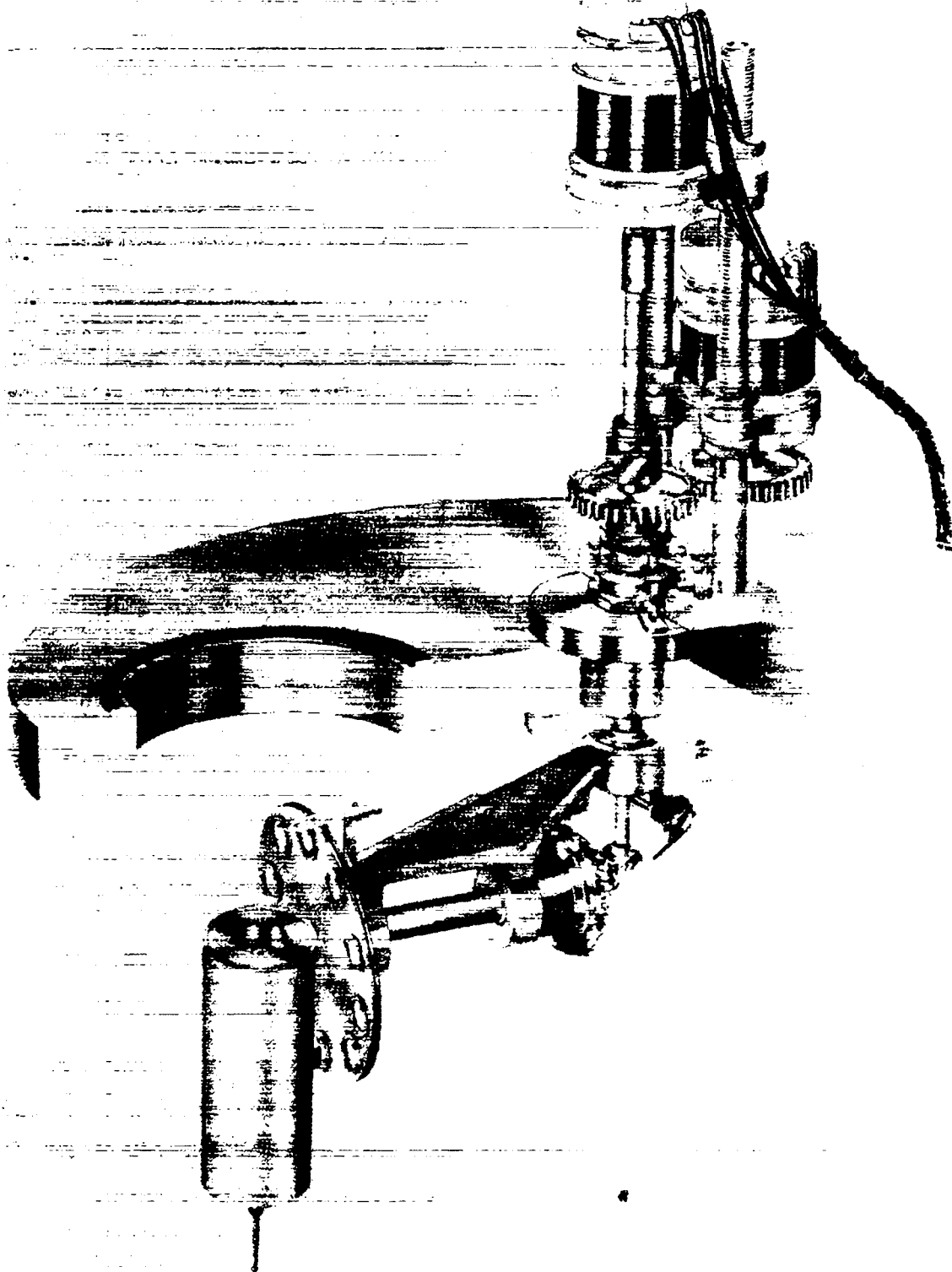


Figure 10

Gas target chamber used with zero degree target.

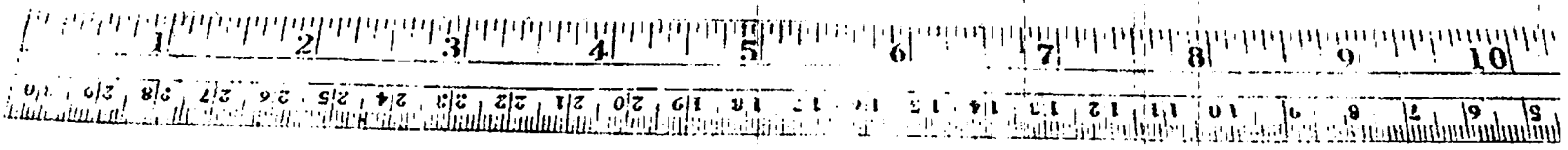
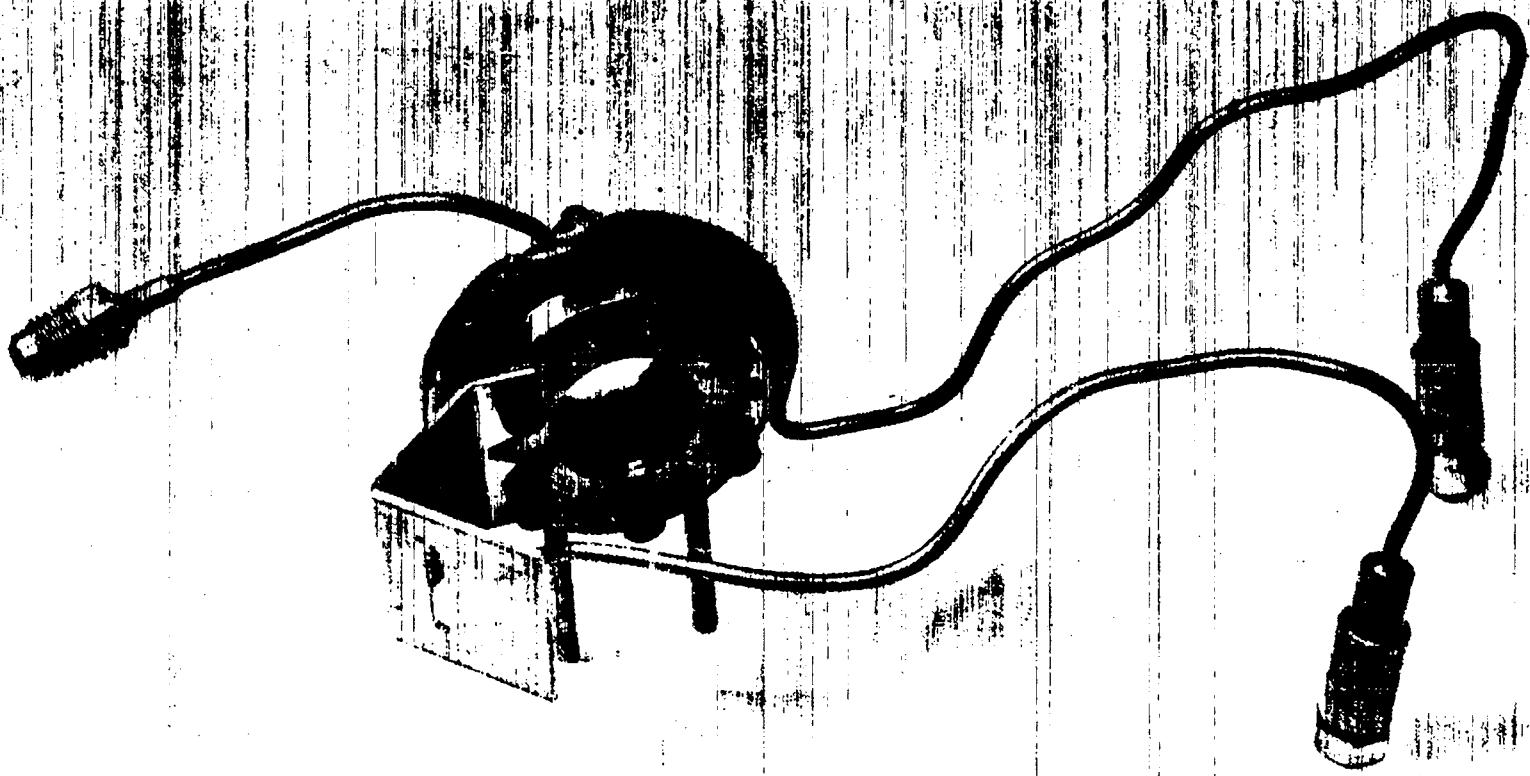


Figure 11  
Auxiliary Faraday cage used with zero degree target.

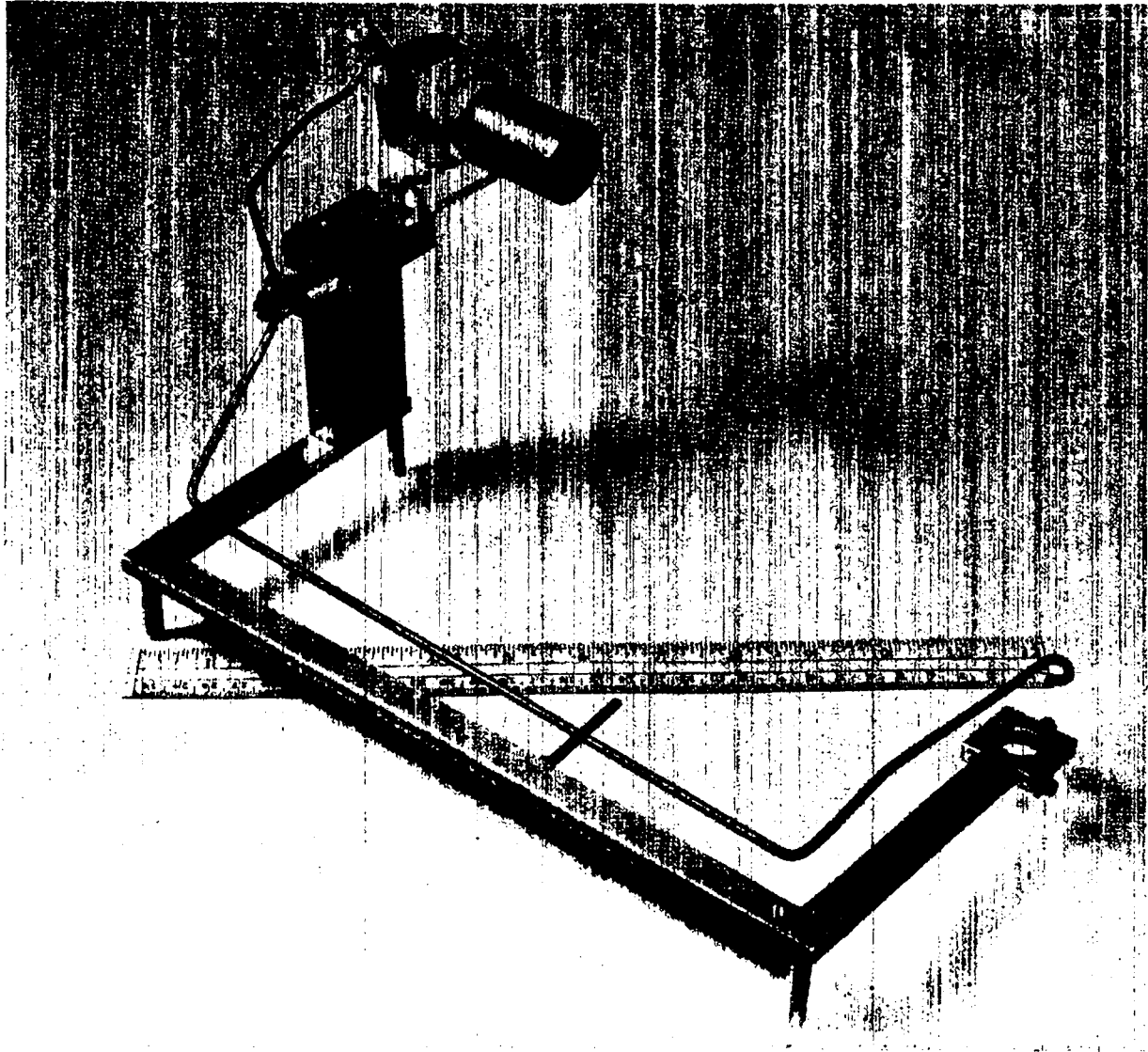
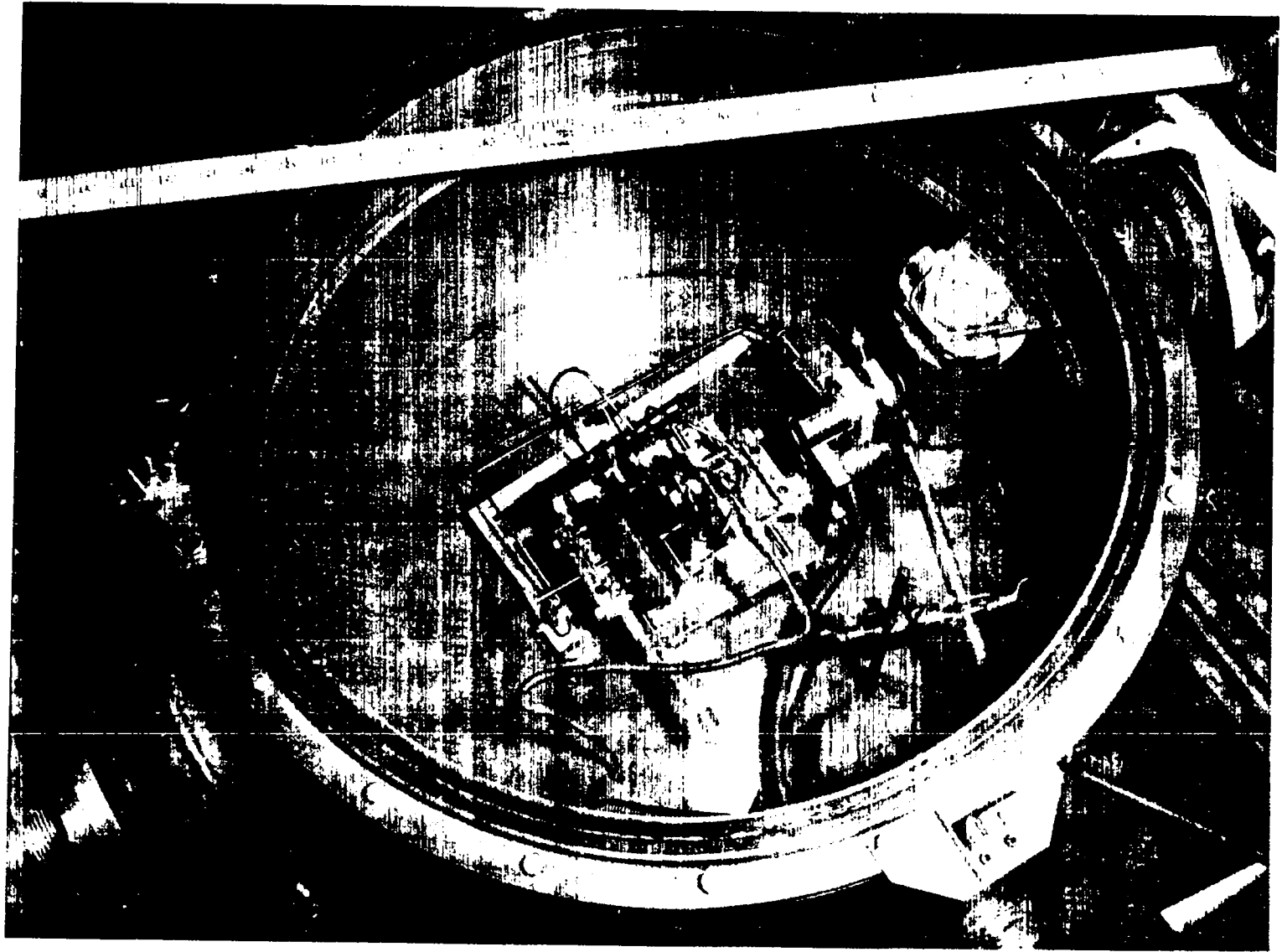


Figure 12  
Reaction chamber arrangement for zero degree point.



order to reduce the rate of reaction particle emission in this prolific direction without having to reduce the target pressure or the beam intensity unduly. The slit on the side of the target (see Fig. 10 -- not shown in Fig. 12) was used for the sole purpose of calibrating the auxiliary Faraday cage.

The auxiliary Faraday cage (Fig. 11) was made much shorter than normal good design would dictate. <sup>20)</sup> This was necessary in order that it could be placed between the counter and the target and still be far enough away from the target so that secondary electrons from the windows gave no trouble. It was mounted so that it could be rotated into the path of the beam from the outside of the reaction chamber. This, too, was for calibration purposes. The back end of the Faraday cage was made of platinum and aluminum foils of such a thickness that protons emitted from the  $D(d,p)H^3$  reaction were able to pass through them into the counter behind with just enough energy to reach the far side of the counter, thus fulfilling the condition of maximum energy loss in the counter mentioned above. Deuterons, on the other hand, were stopped, thereby allowing the deuteron beam current to be measured.

The calibration of the auxiliary Faraday cage was obtained in the following way: first a peak run and then a background run were made in the normal manner counting  $He^3$  particles from the reaction

---

20) Faraday cages whose lengths are not large compared to their diameters may be quite inaccurate because of charge gain resulting from secondary and recoil electron emission. The above auxiliary Faraday cage was found to be gaining about 10.8 percent of its charge in this way.

D(d,n)He<sup>3</sup>. For these runs the counter was set at 43°. Next, the set of runs was repeated with the auxiliary Faraday cage swung into position. The difference in the number of He<sup>3</sup> particles per coulomb of beam current as obtained by these two methods gave directly the calibration of the auxiliary Faraday cage. These calibration runs were repeated several times. Results are tabulated in Table III.

TRIAL	COUNTS PER COULOMB BEAM		CORRECTION INDICATED
	OLD CUP	NEW CUP	
I	48.4	43.0	12.7 %
II	43.7	39.6	10.2
III	47.0	42.8	9.8
IV	47.2	42.8	10.3
V	47.8	43.1	11.0

---

av = 10.8 %

TABLE III

## CHAPTER III

### PROCEDURE

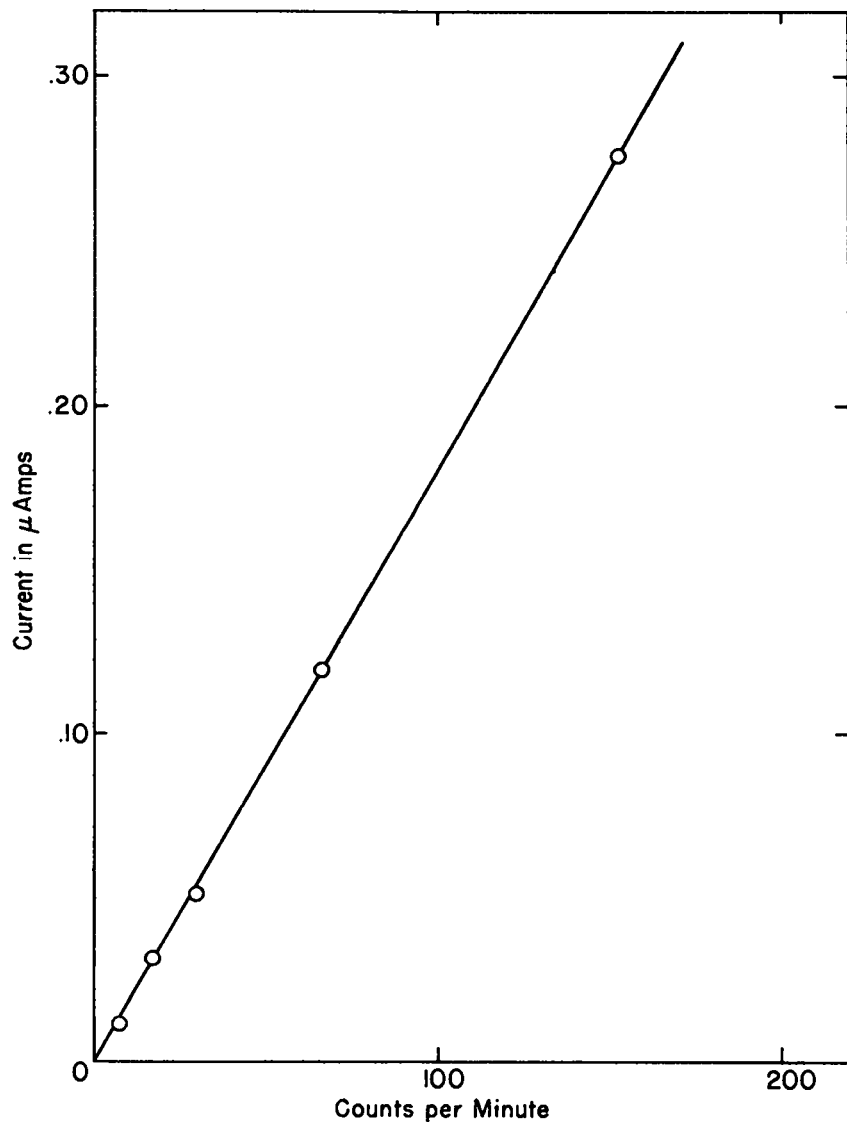
#### A. ANGULAR DATA

The procedure used in taking all the data in this experiment, (including that taken for the zero degree point) was roughly the same. At the start of any half-day's run (i.e., at the start of work in the morning, just after noon, and at the beginning of the night shift,) the ten channel pulse amplitude analyzer and the current integrator were calibrated. The calibration of the ten channel analyzer was made by means of a pulse generator; the height of the pulses was varied linearly across the operating range of the ten channel analyzer. Thus, the relative number of pulses recorded in each of the nine channels was directly proportional to the width of the channel. If any channel recorded a number of counts which differed by more than 10.0 percent from the average, that channel was adjusted and the calibration retaken. It was, of course, not possible to adjust all channels to precisely the same width; therefore, it was always necessary to use this calibration to correct the experimental data taken on this instrument. This correction assisted in making the ten channel analyzer curves smooth and thereby facilitated more accurate background correction.

The calibration of the current integrator was made by allowing a known charge to flow through resistors which by-passed the Faraday

cage and noting the number of current integrator counts so obtained. Internal leakage in the current integrator made it necessary to calibrate at several values of current. Figure 13 is a typical current integrator calibration. After these calibrations were completed the cyclotron was started and, after a sufficient warm up time, a beam was obtained. During this warm up period the counter and target were flushed and filled and the foil system adjusted roughly to that expected to just allow the protons to traverse the counter. During the early part of the experiment when the counter pressure was usually held to values of about  $15\#/in.^2$  or less, this calculated value of the foil adjustment was usually used in the experiment without further check. However, with later data which were taken with up to  $52\#/in.^2$  in the counter, a fine adjustment of the foil system was possible using the cyclotron beam. This was done by watching the position of the peak of the reaction particles on the ten channel pulse amplitude analyzer -- that is, watching which of the channels was counting at the greatest rate, and adjusting the foils to cause this peak to occur at the highest voltage (i.e., at the highest numbered channel) for the particular voltage-pressure ratio being used. This, of course, meant that for the counter pressure being used and within the range of foils available, the maximum possible energy was being lost in the counter by the protons. After the foils were adjusted, the cyclotron beam was usually turned off long enough to allow accurate reading of the target pressure and temperature. A beam was then obtained and, provided the beam intensity was reasonably steady,

Figure 13  
Typical current integrator calibration curve.



a data run was taken, usually of 128 current integrator counts (about 14 microcoulombs.) The readings of the ten channel analyzer and current integrator were taken down at the end of the run, the foils readjusted in order to completely cut out all protons, and a background run taken. On occasion, especially when the cyclotron was running poorly, a background run would be taken both before and after the peak run, thus compensating to some extent for a shift in background during the course of a series of runs. At least once and, on occasion, several times during the day, the beam energy was measured. When the energy was to be measured the cyclotron was not usually turned off between the last series of data runs and the energy measurements. After the energy runs, the cyclotron was turned off, and the target pressure and temperature remeasured. The proportional counter was then adjusted to a new angle, and the same procedure repeated for the next point.

A number of times during the experiment several peak runs were taken at the same angle using various values of stopping foils, all of which were calculated to be thin enough to permit all reaction protons to pass through or beyond the counter. Table IV shows the results of this test. The values appear to vary in a random manner and fall well within the expected accuracy for the points.

#### B. ZERO DEGREE DATA

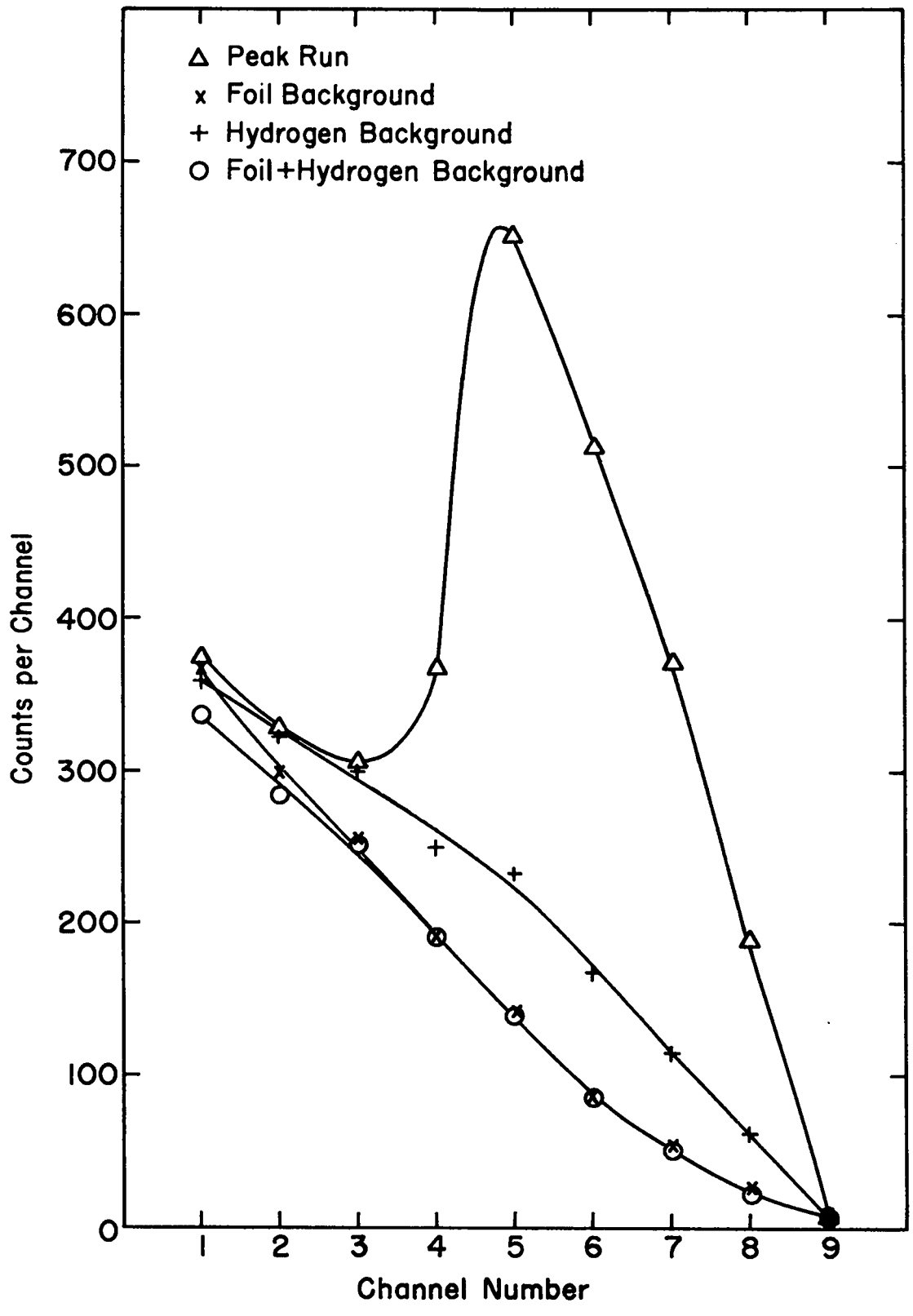
The main data were taken for the zero degree runs in the same manner as for the angular points, except that the background runs were made by filling the gas chamber with hydrogen instead of readjusting the foils. Figure 14 shows the reason for this. It was seen that

LAB ANGLE	FOIL CHANGE	$\sigma(\theta)$ DIFFERENT FROM AVERAGE
22°	0.0 %	+ 1.6 %
	6.6 %	- 1.6 %
32.5°	0.0 %	+ 1.3 %
	4.1 %	- 2.1 %
	8.0 %	+ 0.7 %
	0.0 %	+ 0.3 %
	0.0 %	+ 2.0 %
90°	50.0 %	- 3.4 %
	50.0 %	- 0.0 %
	50.0 %	- 0.3 %
	100.0 %	- 2.3 %

TABLE IV

Figure 14

Ten channel curves obtained at zero degrees using various background combinations.



the foil background was considerably lower than the hydrogen background. It appeared from this that the foils were cutting out some background particles (perhaps formed by deuteron reactions in the nylon windows) which the hydrogen background did not eliminate. Thus the foil background gave too low a value for the background counts and therefore too high a value of the cross section. The background was again too low when the foils were set to take a foil background run and the target was also filled with hydrogen, but this effect was not a function of the hydrogen pressure in the target. This difficulty was not found to be present for angular points, probably because at no time for these points was the counter permitted to see the nylon where it was being bombarded by the main beam.

CHAPTER IV  
DATA ANALYSIS

The fundamental data obtained in the runs above amounted to the number of counts recorded in each of the ten channels of the ten channel pulse analyzer plus those in the total channel, the number of current integrator counts plus the running time, the angular position of the counter, and the target temperature and pressure. The data from the ten channels of the pulse amplitude analyzer for both the peak and background runs were first checked to make sure that the total channel contained essentially the same number of counts as the sum of channels one through nine plus the surplus channel. These data were then normalized to equal beam charge and for variations in channel width as discussed in Chapter III and plotted as number of counts vs. channel number. (See Figures 15, 16, and 17.) The circles are peak run points while the crosses are from background runs.

In some instances, (about half of the time) the background in the counter remained essentially the same for both the peak and background runs. This fact was evidenced by the coincidence of the two curves at the lower channels (see Fig. 15.) In these cases the background correction amounted to no more than a numerical subtraction of the total channels of the two runs. In other cases, however (Fig. 16) the background varied enough during the course

Figure 15

Typical ten channel analyzer curves  
requiring no background correction.

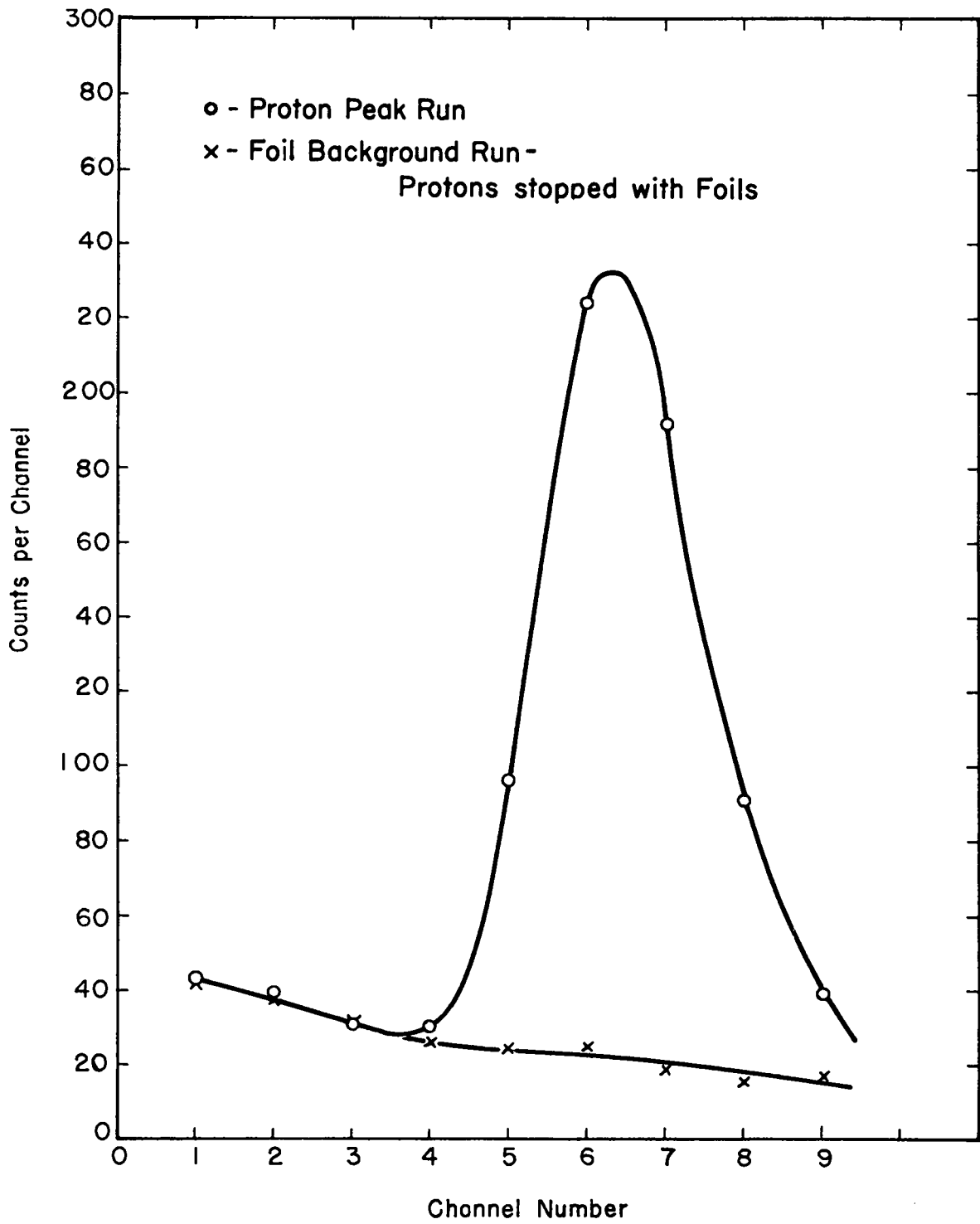


Figure 16

Typical ten channel analyzer curves requiring background correction.

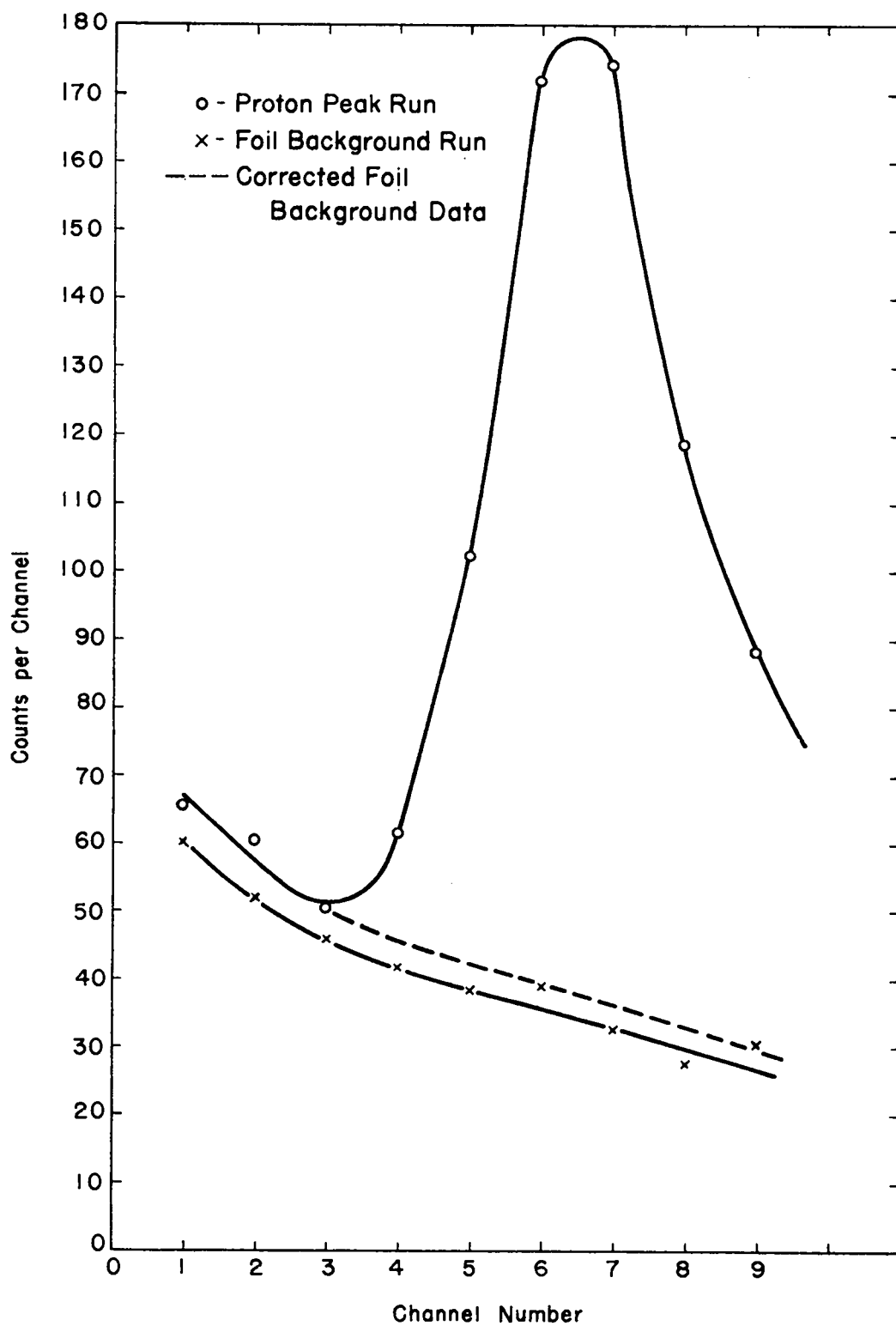
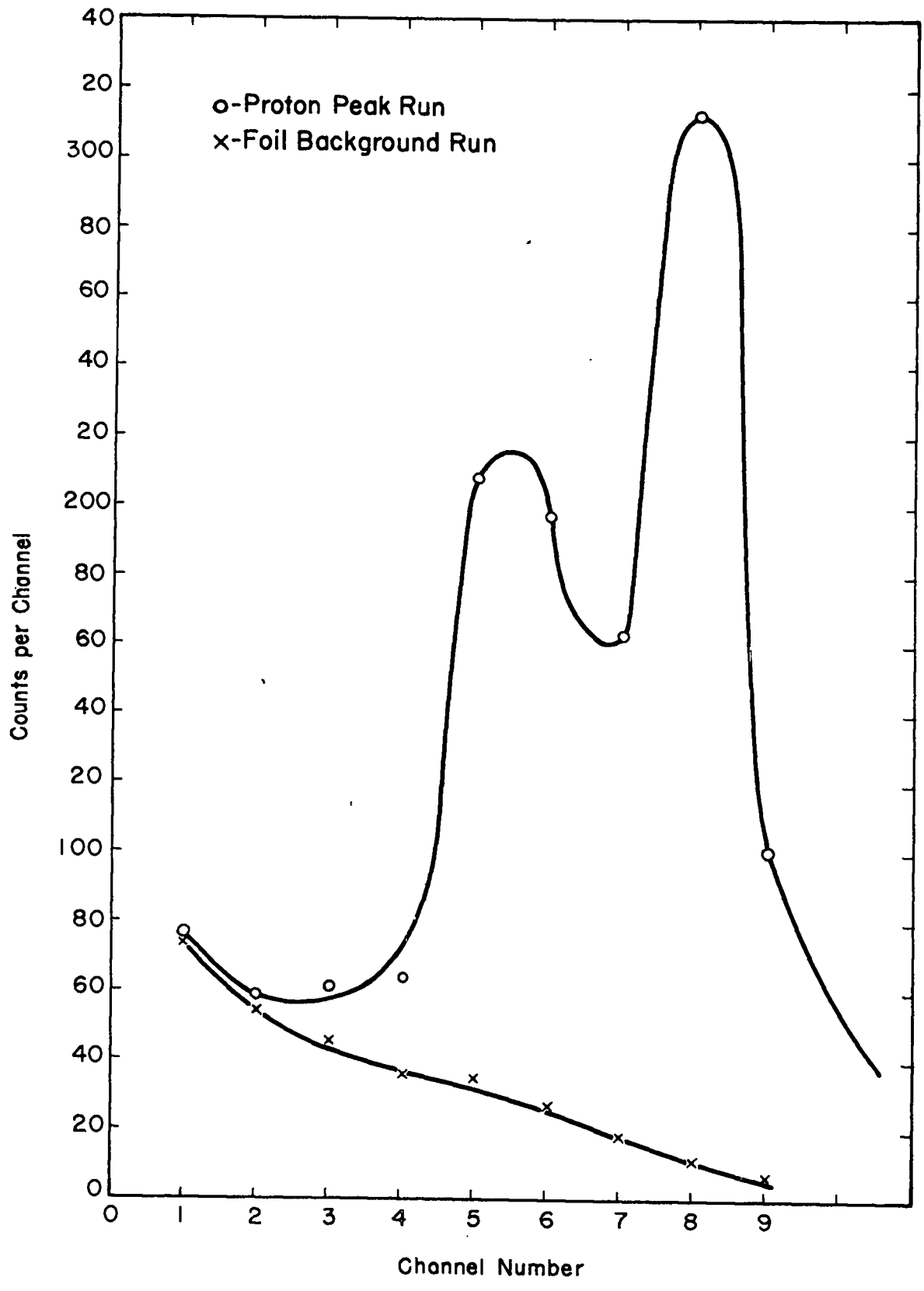


Figure 17  
Ten channel analyzer curves showing  
effect of beam shift.



of the runs so that the background and peak runs did not tie in at the low voltage end. In these cases, the correction was made by raising or lowering the background curve by a constant multiplying factor of the proper amount to make the curves tie in at the desired point (see dotted curve on Fig. 16.) A comparison between this corrected background and the original peak data yielded the number of reaction protons which passed through the counter.

It is worth mentioning that, in the absence of other information, a separation between the peak and background curves, such as is shown in Fig. 16, could be either an indication of the presence of a particle of longer range than the D-D protons which was partially, but not completely, cut out or an indication of a shorter range particle which was cut out of the background but not out of the peak run. Had either of these possibilities been present, the above background treatment would probably have been incorrect; however, both require that the error be fairly constant for repeated runs with the same foil setting and counter pressure. On the contrary, this error seemed to be a completely random effect often disappearing completely from repeat runs of a point. It is therefore concluded that the background shift was real, probably caused by a shift of the internal beam in the cyclotron which, in turn, changed the neutron and gamma background in the counter. This same effect has been noted on occasion when successive background runs were taken under the same conditions of foil setting, counter pressure, etc.

Figure 17 shows a sample of an effect obtained from several

of the runs toward the end of the experiment. If the double peak were a true indication of the range of the proton from the D-D reaction, it would indicate that the triton nucleus had been left in an excited state. Such, however, is almost certainly not the case. The same points taken a few weeks earlier resulted in the usual single peak. The two peaks are believed to be due to an angular shift of the cyclotron beam during the peak run. It has been calculated that a shift of  $\pm 0.3^\circ$  (which was easily permitted by the slit system) would account for the energy separation of the two peaks.

In order to find out accurately the number of deuterons which passed through the target during any particular run, it was usually necessary to note, not only the number of current integrator counts during this run, but the length of time expired. Then, with the counting rate of the current integrator known, it was possible to use the current integrator calibration curve (see Fig. 13) to obtain the total amount of charge per current integrator count at this rate, and hence, obtain the number of deuterons which passed through the counter. This indirect method of calibration was made necessary by the fact that the calibration curves usually did not pass through the origin. In those cases where it did, a constant ratio of coulombs per count was used for all counting rates.

The calculation of the cross section was made by means of the equation:

$$\sigma(\Omega) = K \frac{N(\theta) T F(\theta, \Omega)}{p G \sin \theta} \quad (4)$$

where:  $K/G$  is a constant depending in part on secondary geometry

$N(\theta)$  is the number of protons counted per microcoulomb

$T$  is the target temperature

$p$  is the target pressure

$F(\theta, \alpha)$  is the intensity conversion factor between the Lab.

and center of mass systems

$\theta$  is the Lab. angle to the beam.

This equation is derived in Appendix A - Part I.

The data for the zero degree point were handled in the same manner as for the angular points (see Fig. 14.) The secondary slit system was quite different, however, so that a slight modification of the derivation of the cross section equation (4) was needed (see Appendix A - Part II.)

After all of the data were calculated and plotted, it was found that the resulting curve was not quite symmetrical. All points above  $110^\circ$  center of mass were from four to ten percent higher than their complements on the other side of  $90^\circ$ . It is difficult to see how a reaction involving equal initial masses could give rise to a reaction which would be anti-symmetric in the center of mass system. It is only necessary to consider that, in the center of mass system, two bombarding particles are approaching a fixed central point with identical velocities to realize the absurdity of the question.

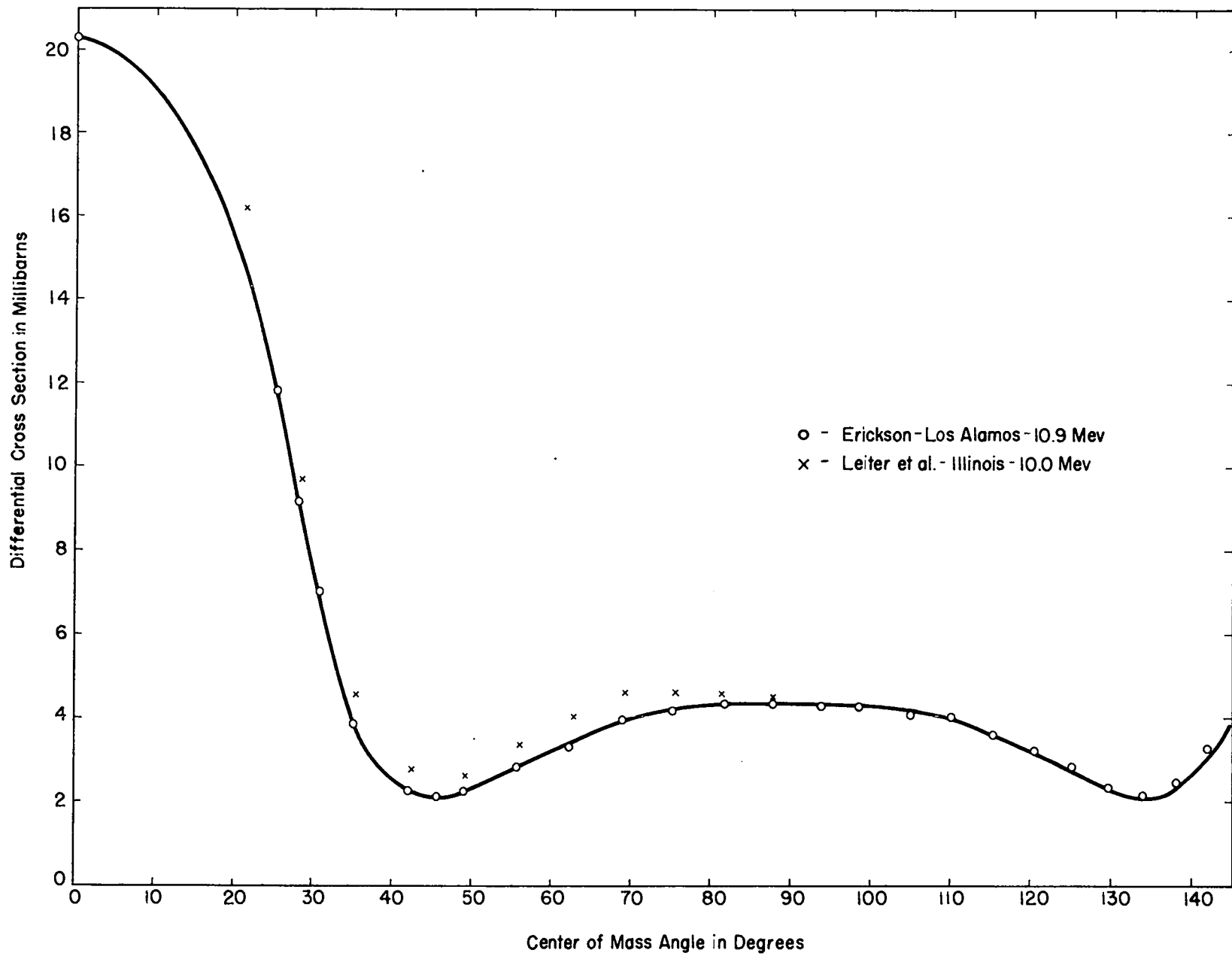
A thorough check of all techniques and calculations and a study of the ranges of particles elastically scattered from various

nuclei revealed several pertinent facts. In the first place, deuterons scattered elastically from  $O^{16}$  or  $N^{14}$  had roughly the same range in the back quadrant as the protons being counted; in the second place, the foil adjustments were such that, at all points in question, deuterons so scattered would produce peaks which probably would not have been separated from the proton peaks; third, at two angles where repeat points were taken with and without the use of the palladium valve to fill the target, the palladium valve data were considerably lower (4.1 percent and 7.6 percent); fourth, a mass spectrograph analysis of deuterium gas received from the producer in the same shipment as that used during the present experiment showed 0.3 percent nitrogen and 0.05 percent oxygen; and finally, a calculation of the  $D-N^{14}$  elastic cross section needed to produce the noticed effect produced a value of 0.04 barns, which is not an unreasonable value.

Although a search of the literature failed to reveal a value for the cross section in question to compare with the 0.04 barns, the four points mentioned above seemed to be sufficient evidence to permit a correction to be made. The correction (5.8 percent) was obtained by averaging the difference between the palladium valve data and the non-palladium valve data and was applied uniformly to all non-palladium valve points taken at greater angles than  $100^\circ$  center of mass.

The resulting data are symmetrical well within the range of the estimated errors. The final data are given in Appendix D and plotted in Fig. 18. The solid curve drawn through the points is

Figure 18  
Differential cross section of D(d,p) T reaction.



symmetrical. The lack of symmetry of the data may be seen in the fact that the curve does not quite represent the best fit to the individual points. Crosses show the  $D(d,p)T$  differential cross section as recently measured by Leiter and others<sup>14)</sup> at Illinois. This work was done by means of nuclear plates at 10.0 Mev as opposed to the present work with counters at 10.9 Mev. Lack of knowledge of the energy dependence of the cross section prevents a comparison.

The standard random error of the individual points is estimated to be  $\pm 1.5$  percent for points below  $100^\circ$  center of mass and  $\pm 2.5$  percent for points above that value. These values were obtained by a comparison of the results of several different analyses. These included a study of values obtained at four points ( $0^\circ$ ,  $20^\circ$ ,  $75^\circ$ , and  $90^\circ$  Lab.) each of which were taken four or more times; a study of the fit of the points to the curve drawn; and a study of the estimated standard errors of various factors which contributed to the accumulated error. The random errors are composed both of items which were purposely varied during the experiment such as secondary geometry, target gas pressure, and stopping material in the secondary path; and of uncontrolled random effects such as those in the current integrator, beam energy, beam direction, target temperature, and counter background conditions. The systematic error is estimated to be  $\pm 2.5$  percent for points below  $100^\circ$  center of mass and  $\pm 3.2$  percent for points above that value. The additional  $\pm 2$  percent error at the larger angles is introduced by uncertainties in the 5.8% correction made to these values in the case of the D-N and D-O

scattering difficulties. The accumulated standard error of the individual points is therefore calculated to be  $\pm 3$  percent for points between zero degrees and  $100^\circ$  center of mass and  $\pm 4$  percent for points at greater angles.

A least-squares fit of this curve in terms of a  $\cos^2\theta$  series was made by the Los Alamos computing division. Equation (5) shows the result of this analysis.

$$\begin{aligned} \sigma(\Omega) = & 4.28 (1 + 1.90 \cos^2 \Omega - 40.07 \cos^4 \Omega + 206.50 \cos^6 \Omega \\ & - 501.50 \cos^8 \Omega + 564.26 \cos^{10} \Omega - 227.34 \cos^{12} \Omega \end{aligned} \quad (5)$$

This equation has some theoretical interest. Since the elastic scattering cross section from Born's theory<sup>21)</sup> has terms containing Legendre polynomials  $(P(\cos \theta))^2$ , it follows from Equation (5) that partial waves up to and including those with angular momentum equal to (5) are probably involved in the reaction. While the above argument is made for elastic scattering, and the present reaction is by no means of this type, it would not be expected that the positive Q<sup>22)</sup> would effect the angular momentum relation. Since workers using energies below 4.0 Mev have required as high as  $\cos^6\theta$  for this reaction, energy extrapolation to 11 Mev indicates that the  $\cos^{12}\theta$  required in the present experiment is consistent.

The total cross section for this reaction, obtained by integrating the cross section curve (Fig. 17) over all space, has been

---

21) H. A. Bethe, Elementary Nuclear Theory (New York, 1947), p. 37, or N. F. Mott and H. S. W. Massey, The Theory of Atomic Collisions (Oxford, 1933), Chapter VII.

22) G. T. Hunter and H. T. Richards, Phys. Rev. 75, 335 (1949).

calculated and found to be 0.063 barns. This value compares as well as can be expected with the 0.07 barns obtained by Erickson, Fowler, and Stovall<sup>13)</sup> at 10.3 Mev for the competing reaction and the 0.075 barns obtained for the present reaction at 10.0 Mev by Leiter.<sup>14)</sup>

## APPENDIX A

### DERIVATION OF EQUATION FOR CALCULATING CROSS SECTION

#### 1. Angular Data

The total cross section for a particular reaction which a single nucleus presents to a beam of  $N$  particles per  $\text{cm}^3$  moving with a velocity  $V$  may be defined by the relation

$$y_T = NV\sigma_T \quad (1)$$

where  $y_T$  is the total yield from the reaction per nucleus being bombarded. If we wish to consider yield per unit solid angle  $y(\theta)$  and the cross section per unit solid angle  $\sigma(\theta)$  (i.e., differential cross section) we have

$$y(\theta) = NV\sigma(\theta) \quad (2)$$

Now, if we multiply the right side of this equation (2) by  $n$  particles per  $\text{cm}^3$  in the "target", by the volume of the gas being bombarded ( $\ell \times A$ ), and by a solid angle  $a/R^2$ ; then, the yield  $y(\theta)$  becomes  $Y(\theta)$ , the number of particles emitted into the solid angle  $a/R^2$  per unit time for all nuclei in the path  $\ell$  of the beam.

We can define the quantity

$$\eta(\theta) = \frac{Y(\theta)}{NVAC} \quad (3)$$

If  $C$  is the charge per bombarding particle, then  $\eta(\theta)$  is the yield per beam charge.

We can express the  $n$  of the above paragraph in terms of more immediately useful factors.

$$n = K \frac{p}{T} \quad (4)$$

Where  $p$  and  $T$  are the pressure and temperature of the gas target and  $K$  is a constant including Avagadro's number.

When we take the above factors into account, the equation for the differential cross section becomes

$$\sigma(\theta) = \frac{n(\theta) C T}{K p} \cdot \frac{R^2}{l a} \quad (5)$$

We will denote the geometrical factor  $l a / R^2$  by  $G'$  and combine  $K = C/K$

Then

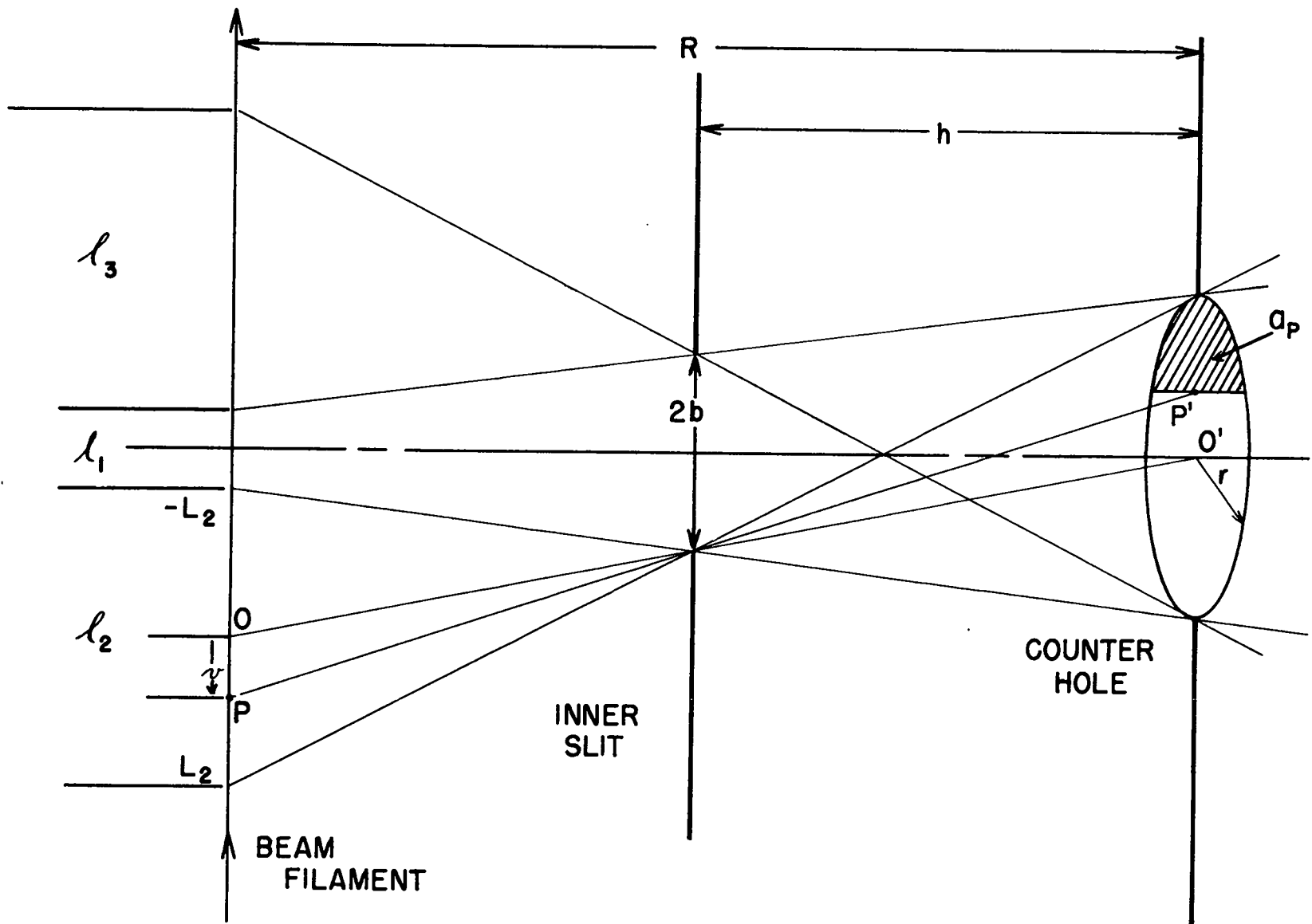
$$\sigma(\theta) = K \frac{n(\theta) T}{p G'} \quad (6)$$

In order to use this equation with the secondary slit system used in this experiment, certain corrections must be made to the factor  $G'$ . These corrections stem from the fact that, at some points in the target gas, the solid angle for reaction particle emission is defined by only part of the counter window. Figure A-1 shows the difficulty. A particle at  $P$ , for example, can see only the cross-hatched portion of the counter window, and its corresponding solid angle is defined by this new area divided by  $R^2$ .

Before starting to treat this problem, we should point out that the actual ratio of the counter hole radius to the distance between the counter and the beam was never greater than 0.02, so that assumptions such as the constancy of the distance between all points

Figure A - 1

Diagram used in derivation of cross section equation.



on the counter hole area and all points on the beam filament are really valid.

Suppose the counter is set at  $90^\circ$  to the beam in the laboratory system and consider only a single filament of the beam trajectory - say at the center of the beam. Divide this beam filament into three regions ( $l_1, l_2,$  and  $l_3$ ) defined by the intersection of lines along the extremities of the inner slit and counter hole with the beam filament, as shown in Fig. A-1. Now it is easily seen that particles in region  $l_1$ , will have the normal  $a/R^2$  solid angle associated with them, while those in  $l_2$  and  $l_3$  will see only part of the counter hole area  $a$  and will therefore have an associated solid angle somewhat less than  $a/R^2$ .

The area of the counter hole which can be seen from any point in  $l_2$ , say from point P, can be easily obtained by integrating an element of area over the counter hole and using as a lower limit the intersection with the counter hole of a plane through P and the inner slit edge.

This integration, divided by  $R^2$  to give it dimensions of a solid angle, yields

$$\frac{a_p}{R^2} = \frac{\pi r^2}{2R^2} - \frac{1}{2R^2} \left[ kv \sqrt{r^2 - kv^2} + r^2 \sin^{-1} \left( \frac{kv}{r} \right) \right] \quad (7)$$

where  $v$  is a coordinate indicating the position of P and  $k = \frac{h}{R-h}$ .

The various symbols are defined in Figure A-1.

Now if we multiply by  $dv$  and integrate this expression over the

region  $l_2$  (i.e., from  $-L_2$  to  $+L_2$ ), we find that the average solid angle for all points in region  $l_2$  is

$$\frac{\bar{a}_p}{R^2} = \frac{\pi r^2}{2R^2} = \frac{a}{2R^2} \quad (8)$$

where  $a$  is, as before, the total counter hole area.

This result means that the solid angle subtended by the counter for reactions taking place in  $l_2$  and  $l_3$  is, on the average, one-half that for reactions taking place in  $l_1$ . Thus, the  $G'$  equation (6) may be replaced by

$$G = \frac{2L_1 a}{R^2} + \frac{1}{2} \left( \frac{2L_2 a}{R^2} + \frac{2L_3 a}{R^2} \right) \quad (9)$$

where  $2L_1$ ,  $2L_2$ , and  $2L_3$  are the lengths of regions  $l_1$ ,  $l_2$ , and  $l_3$  respectively.

Straightforward geometrical considerations yield

$$L_2 = L_3 = \frac{R(r+b) - h(r-L_1)}{h} \quad (10)$$

$$L_1 = \frac{Rb - Rr + hr}{h} \quad (11)$$

Combining equations (9), (10), and (11), we obtain

$$G = \frac{2ab}{Rh} \quad (12)$$

which, as mentioned above, should be put in place of  $G'$  in equation (6).

If the counter is set at some angle other than  $90^\circ$  lab., then  $L_1$ ,  $L_2$ , and  $L_3$  are all lengthened by an amount  $\frac{1}{\sin \theta}$ , so that

finally equation (6) becomes

$$\sigma(\theta) = K \frac{\eta(\theta) T}{p G \sin \theta} \quad (13)$$

This equation may be expressed in center of mass coordinates by multiplying it by the ratio of intensities in the two systems which we will call  $F(\theta, \Omega)$ . This factor will be derived in Appendix B.

Then, the cross section equation in center of mass system is

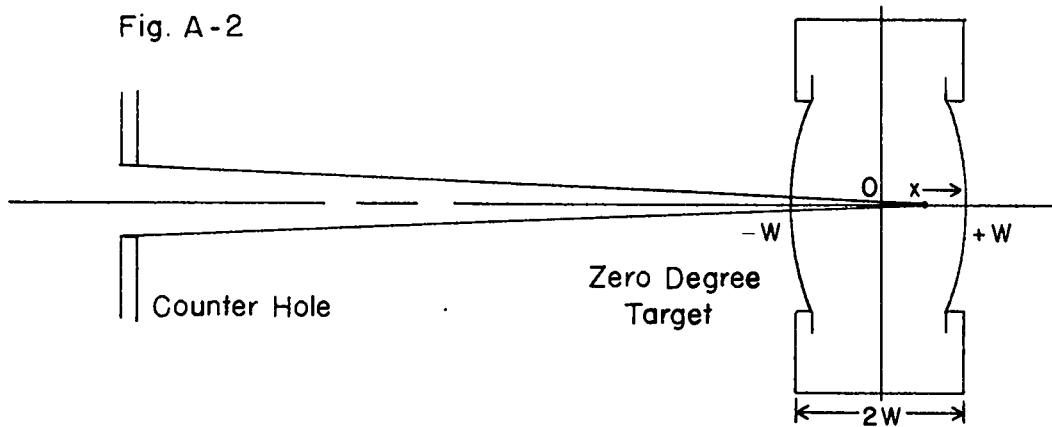
$$\sigma(\Omega) = K \frac{\eta(\theta) T F(\theta, \Omega)}{p G \sin \theta} \quad (14)$$

This derivation ignores several errors such as those caused by finite beam size and variation of  $R$  with  $L$  when  $\theta \neq 90^\circ$ . These errors have been checked graphically and found to be much too small to give trouble. The most reliable check of the validity of this equation lies in the fact that a factor of two change in the secondary geometry resulted in no measurable systematic change in the calculated cross sections.

## 2. Zero Degree Data

For the zero degree point, the inner slit of the secondary slit system was removed, so that the complicated solid angle geometry calculations of the previous section are not necessary. In this case, however, the reactions can take place at distances from the counter which vary by as much as  $\pm$  five percent, so a correction term was put in to take care of this effect.

Fig. A-2



The problem here is to integrate the solid angle subtended by the counter along a beam filament with the two target windows as limits of integration. Thus, the average solid angle

$$\omega = \frac{a}{2W} \int_{-W}^{+W} \frac{dx}{(R+x)^2} = \frac{a}{2W} \left[ \frac{2W}{R^2 - W^2} \right] \quad (15)$$

and in the terms of the previous work  $2w - l_1$ , the length of the target path, so the  $G$  of equation (14) becomes

$$G = \frac{la}{R^2 - (l/2)^2} \quad (16)$$

With this change in  $G$  equation (14) is used for the zero degree point.

## APPENDIX B

### TRANSFORMATION RELATIONS BETWEEN LAB. AND CENTER OF MASS SYSTEMS

Consider a compound nucleus of mass four disintegrating, in the center of mass system, into two nuclei of mass three and mass one respectively. While the masses of the compound D-D nucleus, the triton, and the proton are not precisely in the ratio of 4:3:1, they are close enough for our purposes.

Due to the laws of conservation of momentum, the two particles will be emitted in diametrically opposite directions. In other words,  $\theta_p = 180 - \theta_t$  where the subscripts p and t refer to protons and tritons and the unbarred  $\theta$ 's are center of mass angles to the beam.

Now adding components of the velocity of the triton particle.

$$\bar{v}_t \cos \bar{\theta}_t = \bar{V} - v_t \cos \theta_t \quad (1)$$

$$\bar{v}_t \sin \bar{\theta}_t = v_t \sin \theta_t \quad (2)$$

from which

$$\tan \bar{\theta}_t = \frac{v_t \sin \theta_t}{\bar{V} - v_t \cos \theta_t} \quad (3)$$

where the barred symbols refer to the lab system and  $\bar{V}$  is the velocity of the center of mass with respect to the lab system.

Now, because of the fact that the bombarding particle and the target particle are of equal mass (i.e., both deuterons), the center of mass velocity is just 1/2 of the original deuteron velocity or

$$\bar{V} = \frac{\bar{v}_d}{2} \quad (4)$$

and the velocity of the bombarding deuteron expressed in terms of its energy is

$$\bar{E}_d = \frac{1}{2} m_d \bar{v}_d^2 \quad (5)$$

$$\bar{v}_d = \sqrt{2\bar{E}_d/m_d} = 2V \quad (6)$$

Now in the center of mass system the deuterons approach each other with a velocity  $v_d = \bar{V}$  and each has an energy,

$$E_d = \frac{1}{2} m_d v_d^2 = \frac{1}{2} m_d \bar{V}^2 \quad (7)$$

Therefore, the total energy going into the collision in the center of mass system is

$$E_0 = m_d \bar{V}_d^2 = \frac{m_d \bar{v}_d^2}{4} \quad (8)$$

but the total original energy (i.e., that of the original deuteron) was

$$\bar{E}_d = \frac{m_d \bar{v}_d^2}{2} = 2E_0 \quad (9)$$

Thus one-half of the total bombarding energy goes into recoil particles in the center of mass system while the other half goes into the motion of the center of mass with respect to the lab system.

From the laws of conservation of energy and momentum,

$$\frac{1}{2} m_t v_t^2 + \frac{1}{2} m_p v_p^2 = Q + E_0 \quad (10)$$

and

$$m_t v_t = m_p v_p \quad (11)$$

where  $Q$  is the difference in binding energies between the two conditions (i.e., two deuterons vs a triton and a proton.)

Combining (10) and (11) we obtain

$$v_p = \frac{m_t}{m_p} v_t \quad (12)$$

and

$$v_t = \sqrt{\frac{2Q + \bar{E}_d}{m_t + m_t^2/m_p}} \quad (13)$$

These two equations can now be used together with equation (4) in equation (3) to obtain the value of center of mass angle for a particular lab angle.

In order to be consistent with the other work in this paper, we will leave the barred and unbarred systems and let

$$\begin{aligned} \bar{\theta}_t &= \phi & v_t &= v_t \\ \bar{\theta}_p &= \theta & v_p &= v_p \\ \theta_p &= \gamma = 180^\circ - \theta_t & \bar{V} &= V \\ \bar{E}_d &= E_d & \bar{v}_d &= v_d \end{aligned} \quad (14)$$

then we have

$$\tan \phi = \frac{v_t \sin(180^\circ + \gamma)}{V - v_t \cos(180^\circ + \gamma)} \quad (15)$$

where  $V = \frac{V_d}{2}$

(16)

and similarly

$$\tan \theta = \frac{v_p \sin \delta}{V - v_p \cos \delta} \quad (17)$$

$$v_t = \sqrt{\frac{2Q + E_d}{m_t + m_t^2/m_p}} \quad (18)$$

$$v_p = \frac{m_t}{m_p} v_t \quad (19)$$

As was mentioned in Appendix A, to transform a cross section value from the lab system to the center of mass system requires a factor  $F(\theta, \alpha)$  which depends on the ratio of the solid angles in the two systems. Thus

$$F(\theta, \alpha) = \frac{I(\alpha)}{I(\theta)} = \frac{2\pi \sin \theta d\theta}{2\pi \sin \alpha d\alpha} \quad (20)$$

An expression of  $F(\theta, \alpha)$  in terms of known values may be obtained by performing the operation  $d\theta/d\alpha$  on equation (17) and multiplying the result by  $\frac{\sin \theta}{\sin \alpha}$ . Simplifying, we have

$$F(\theta, \alpha) = \frac{\sin^3 \theta}{\sin^3 \alpha} \left(1 + \frac{V}{v_p} \cos \alpha\right) \quad (21)$$

which is the derived expression.

## APPENDIX C

### RELATIVE STOPPING POWER OF NYLON

In conjunction with the use of nylon window material on the wide angle target, a test was made to determine the relative stopping power of nylon with respect to air.

This was measured by comparing the effect on the length of  $\alpha$ -particle tracks in nuclear plates, of inserting first nylon then air between the plutonium source and the plate.

The nuclear plate was placed at about five deg. to the path of the beam of  $\alpha$ -particles and, in the case of the air run, the air was allowed to fill all the space between the source and the plate. This resulted in a gradual shortening of the track length along this plate away from the source. The nylon, on the other hand, removed, on the average, an equal amount of energy from the  $\alpha$ -particles. It remained only to find at what distance from the source the air-run tracks were equal in length to the tracks from the nylon run. This distance in centimeters of air, corrected to 76 cm Hg pressure and 15°C temperature, is the air equivalence of the nylon foil being tested.

It was determined that, at least under the conditions of this test,

$$1 \text{ mg/cm}^2 \text{ nylon} = 0.93 \text{ cm air.}$$

APPENDIX D - RESULTS

Data Table I - Intermediate Results

Lab	Angle		Counts $\mu$ Coulomb	Target		Deuteron Energy (Mev)	$\omega$ *	$\sigma$ ( $\Omega$ ) (Millibarns)
	CM			P (Gm Hg)	T ( $^{\circ}$ F)			
0 $^{\circ}$	0 $^{\circ}$		1871.0	21.9	63.3	10.13	-	20.4
0 $^{\circ}$	0 $^{\circ}$		1405.0	16.8	64.0	10.13	-	20.4
0 $^{\circ}$	0 $^{\circ}$		1455.0	16.8	64.0	10.13	-	21.0
0 $^{\circ}$	0 $^{\circ}$		1783.0	21.9	63.9	10.13	-	19.9
0 $^{\circ}$	0 $^{\circ}$		1762.0	21.9	63.3	10.13	-	19.6
18 $^{\circ}$	25.3 $^{\circ}$		1306.1	32.1	61.9	10.25	1.9 $^{\circ}$	11.83
20 $^{\circ}$	28.1 $^{\circ}$		2196.4	78.1	61.2	10.17	1.9 $^{\circ}$	9.15
20 $^{\circ}$	28.1 $^{\circ}$		905.9	32.1	61.8	10.26	1.9 $^{\circ}$	9.20
20 $^{\circ}$	28.1 $^{\circ}$		879.7	32.1	62.1	10.26	1.9 $^{\circ}$	8.94
20 $^{\circ}$	28.1 $^{\circ}$		909.1	32.1	62.4	10.26	1.9 $^{\circ}$	9.25
22 $^{\circ}$	30.9 $^{\circ}$		1615.3	82.1	57.4	10.28	1.9 $^{\circ}$	7.11
22 $^{\circ}$	30.9 $^{\circ}$		1583.8	82.1	57.7	10.26	1.9 $^{\circ}$	6.89
25 $^{\circ}$	35.2 $^{\circ}$		269.6	57.5	73.8	10.54	1.9 $^{\circ}$	3.91
30 $^{\circ}$	42.1 $^{\circ}$		383.4	89.4	64.7	10.09	1.9 $^{\circ}$	2.17
30 $^{\circ}$	42.1 $^{\circ}$		406.4	89.4	65.0	10.09	1.9 $^{\circ}$	2.31
30 $^{\circ}$	41.9 $^{\circ}$		617.9	34.8	67.9	11.02	2.7 $^{\circ}$	2.26
32.5 $^{\circ}$	45.5 $^{\circ}$		321.8	89.2	61.0	10.25	1.9 $^{\circ}$	1.99
32.5 $^{\circ}$	45.5 $^{\circ}$		524.0	34.4	68.2	11.02	2.7 $^{\circ}$	2.11

\* $\omega$  = the half angular resolution of the secondary slit system.

Lab	Angle	Counts $\mu$ Coulomb	Target		Deuteron Energy (Mev)	$\omega$ *	$\sigma$ ( $\Omega$ ) (Millibarns)
	CM		P (Cm Hg)	T ( $^{\circ}$ F)			
35 $^{\circ}$	49.0 $^{\circ}$	326.9	86.7	63.8	10.37	1.9 $^{\circ}$	2.27
35 $^{\circ}$	48.8 $^{\circ}$	503.7	34.7	68.7	11.02	1.9 $^{\circ}$	2.19
40 $^{\circ}$	55.7 $^{\circ}$	317.2	78.8	64.7	10.54	1.9 $^{\circ}$	2.83
40 $^{\circ}$	55.7 $^{\circ}$	812.8	51.8	70.2	10.88	2.7 $^{\circ}$	2.78
45 $^{\circ}$	62.3 $^{\circ}$	305.6	78.2	62.4	10.13	1.9 $^{\circ}$	3.15
45 $^{\circ}$	62.3 $^{\circ}$	650.4	39.2	68.6	10.93	2.7 $^{\circ}$	3.37
45 $^{\circ}$	62.3 $^{\circ}$	696.0	39.7	70.2	10.91	2.7 $^{\circ}$	3.56
50 $^{\circ}$	69.0 $^{\circ}$	345.4	81.5	62.1	10.54	1.9 $^{\circ}$	3.89
50 $^{\circ}$	69.0 $^{\circ}$	813.6	48.9	72.3	10.93	2.7 $^{\circ}$	3.88
50 $^{\circ}$	69.0 $^{\circ}$	833.6	47.1	68.8	11.02	2.7 $^{\circ}$	4.10
55 $^{\circ}$	75.3 $^{\circ}$	328.7	80.8	62.9	10.13	1.9 $^{\circ}$	4.24
55 $^{\circ}$	75.6 $^{\circ}$	812.8	52.1	69.9	10.93	2.7 $^{\circ}$	4.10
60 $^{\circ}$	81.7 $^{\circ}$	320.9	80.7	61.6	10.13	1.9 $^{\circ}$	4.63
60 $^{\circ}$	81.8 $^{\circ}$	714.4	51.0	72.4	10.88	2.7 $^{\circ}$	4.15
60 $^{\circ}$	81.7 $^{\circ}$	309.8	80.6	64.4	10.18	1.9 $^{\circ}$	4.50
60 $^{\circ}$	81.7 $^{\circ}$	309.8	80.6	65.0	10.18	1.9 $^{\circ}$	4.50
65 $^{\circ}$	87.8 $^{\circ}$	272.0	80.6	61.7	10.23	1.9 $^{\circ}$	4.39
65 $^{\circ}$	87.8 $^{\circ}$	294.1	84.7	64.6	10.22	1.9 $^{\circ}$	4.55
65 $^{\circ}$	87.8 $^{\circ}$	664.9	52.3	70.1	10.93	2.7 $^{\circ}$	4.20
70 $^{\circ}$	93.8 $^{\circ}$	257.6	84.7	65.1	10.17	1.9 $^{\circ}$	4.42
70 $^{\circ}$	93.5 $^{\circ}$	577.2	52.4	70.2	10.93	2.7 $^{\circ}$	4.03

\* $\omega$  - the half angular resolution of the secondary slit system.

Lab	Angle	Counts $\mu$ Coulomb	Target		Deuteron Energy (Mev)	$\omega$ *	$\sigma$ ( $\Omega$ ) (Millibarns)
	CM		P (Cm Hg)	T ( $^{\circ}$ F)			
70 $^{\circ}$	93.5 $^{\circ}$	563.5	47.3	68.8	11.02	2.7 $^{\circ}$	4.35
75 $^{\circ}$	98.5	229.8	84.8	64.9	10.30	1.9 $^{\circ}$	4.28
75 $^{\circ}$	99.1 $^{\circ}$	532.0	49.5	74.0	10.93	2.7 $^{\circ}$	4.41
75 $^{\circ}$	99.1 $^{\circ}$	480.5	49.3	73.6	10.93	2.7 $^{\circ}$	4.00
75 $^{\circ}$	99.1 $^{\circ}$	429.1	39.5	70.7	10.91	2.7 $^{\circ}$	4.41
75 $^{\circ}$	99.1 $^{\circ}$	429.8	39.5	70.8	10.91	2.7 $^{\circ}$	4.41
80 $^{\circ}$	104.9 $^{\circ}$	204.8	84.7	64.2	10.26	1.9 $^{\circ}$	4.15
80 $^{\circ}$	104.7 $^{\circ}$	508.4	52.5	70.1	10.93	2.7 $^{\circ}$	4.08
80 $^{\circ}$	104.7 $^{\circ}$	456.6	47.4	68.8	11.02	2.7 $^{\circ}$	4.05
85 $^{\circ}$	110.2 $^{\circ}$	195.6	84.6	64.8	10.16	1.9 $^{\circ}$	4.52
85 $^{\circ}$	110.1 $^{\circ}$	419.2	48.3	70.2	10.93	2.7 $^{\circ}$	4.01
90 $^{\circ}$	115.3 $^{\circ}$	133.4	80.5	65.4	10.16	1.9 $^{\circ}$	3.54
90 $^{\circ}$	115.3 $^{\circ}$	456.2	65.9	69.9	10.88	2.7 $^{\circ}$	3.50
90 $^{\circ}$	115.3 $^{\circ}$	471.4	65.7	70.9	10.88	2.7 $^{\circ}$	3.81
90 $^{\circ}$	115.3 $^{\circ}$	466.7	65.4	72.3	10.88	2.7 $^{\circ}$	3.81
90 $^{\circ}$	115.3 $^{\circ}$	453.6	60.4	69.8	10.88	2.7 $^{\circ}$	3.81
90 $^{\circ}$	115.3 $^{\circ}$	419.5	60.0	69.8	10.88	2.7 $^{\circ}$	3.71
90 $^{\circ}$	115.3 $^{\circ}$	437.0	59.8	69.7	10.88	2.7 $^{\circ}$	3.88
95 $^{\circ}$	120.4 $^{\circ}$	344.6	58.8	70.4	10.91	2.7 $^{\circ}$	3.22
100 $^{\circ}$	125.1 $^{\circ}$	279.0	58.6	71.0	10.91	2.7 $^{\circ}$	2.87
105 $^{\circ}$	129.7 $^{\circ}$	215.7	58.4	71.4	10.91	2.7 $^{\circ}$	2.35

\*  $\omega$  = the half angular resolution of the secondary slit system.

Lab	Angle		<u>Counts</u> $\mu$ Coulomb	Target		Deuteron Energy (Mev)	$\omega^*$	$\sigma(\Omega)$ (Millibarns)
	CM			P (Cm Hg)	T ( $^{\circ}$ F)			
105 $^{\circ}$	129.7 $^{\circ}$		279.0	77.6	71.8	10.91	2.7 $^{\circ}$	2.29
110 $^{\circ}$	133.9 $^{\circ}$		266.8	81.8	71.8	10.91	2.7 $^{\circ}$	2.20
110 $^{\circ}$	133.9 $^{\circ}$		227.5	72.4	63.4	11.02	2.7 $^{\circ}$	2.08
115 $^{\circ}$	138.1 $^{\circ}$		272.8	78.5	70.6	10.91	2.7 $^{\circ}$	2.45
120 $^{\circ}$	141.9 $^{\circ}$		350.5	78.2	71.8	10.91	2.7 $^{\circ}$	3.29

\*  $\omega$  = the half angular resolution of the secondary slit system.

Data Table II - Results

Lab < 0	CM < 0	Average ♂ 20.30
18	25.3	11.83
20	28.1	9.13
22	30.9	7.00
25	35.2	3.91
30	42.1	2.25
32.5	45.6	2.05
35	49.0	2.23
40	55.7	2.80
45	62.3	3.35
50	69.0	3.96
55	75.3	4.17
60	81.7	4.35
65	87.8	4.33
70	93.8	4.30
75	98.5	4.29
80	104.9	4.09
85	110.2	4.01
90	115.3	3.60
95	120.4	3.22
100	125.1	2.82
105	129.7	2.32
110	133.9	2.15
115	138.1	2.45
120	141.9	3.28

## BIBLIOGRAPHY

- J. C. Allred, K. W. Erickson, J. L. Fowler, and E. J. Stovall, Jr.,  
"Angular Distribution of 10.8 Mev Deuterons Scattered by  
Deuterons," Physical Review (to be published 1949).
- W. E. Bennett, C. E. Mandeville, and H. T. Richards, "The Yield Function  
and Angular Distribution of the D-D Neutrons," Physical  
Review 69, 418 (1946).
- H. A. Bethe, Elementary Nuclear Theory, New York: John Wiley and  
Sons, Inc., 1947.
- J. M. Blair, G. Freier, E. Lampi, Wm. Sleator, Jr., and J. H. Williams,  
"The Angular Distributions of the Products of the D-D Reaction:  
1 to 3.5 Mev," Physical Review 74, 1599 (1948).
- E. Bretscher, A. P. French, and F. G. P. Seidl, "Low Energy Yield of  
 $D(d,p)H^3$  and the Angular Distribution of the Emitted Protons,"  
Physical Review 73, 815 (1948)
- J. H. Coon, R. W. Davis, A. C. Graves, E. R. Graves, and J. H. Manley,  
"Measurement of the Cross Section for the Reaction  $D(d,p)H^3$ ,"  
LADC 56 (1944) (declassified).
- J. H. Coon, R. W. Davis, E. R. Graves, J. H. Manley, and R. Nobles,  
"Measurement of the Cross Section for the Reaction  $D(d,n)He^3$ ,"  
LADC 75 (1944) (declassified).
- B. R. Curtis, J. L. Fowler, and L. Rosen, "Instrumentation for Nuclear  
Studies with Externally Focused Deuteron Beam from Ten-Mev  
Cyclotron," Review Scientific Instruments 20, 388 (1949).
- E. W. Dexter, "A 10 Channel Pulse Height Analyzer," IAMS 573 (1947)  
(declassified).
- K. W. Erickson, J. L. Fowler, and E. J. Stoval, Jr., "Cross Section  
as a Function of Angle for the  $D(d,n)He^3$  Reaction for 10 Mev  
Bombarding Deuterons," Physical Review (to be published 1949).
- G. T. Hunter and H. T. Richards, "Angular Yield of Neutrons from the  
D-D Reaction," Bulletin American Physical Society 23, No.7,
- R. D. Huntoon, A. Ellett, D. S. Bayley and J. A. Van Allen, "Distribution  
in Angle of Protons from the Deuteron-Deuteron Reaction,"  
Physical Review 58, 97 (1940).

- A. E. Kempton, B. C. Browne, and R. Maasdorp, "Angular Distributions of the Protons and Neutrons Emitted in Some Transmutations of Deuterium," Proceedings Royal Society A157, 386 (1936).
- P. G. Kruger, private communication.
- R. Ladenburg and M. H. Kanner, "On the Neutrons from the Deuteron-Deuteron Reaction," Physical Review 52, 911 (1937).
- H. A. Leiter, R. F. Meagher, F. A. Rodgers, and P. G. Kruger, "Angular Distribution of Protons from the D-D Reaction for 10 Mev Deuterons," Bulletin American Physical Society 24, No 4, 12 (1949).
- N. F. Mott and H. S. W. Massey. The Theory of Atomic Collisions. Oxford: the Clarendon Press, 1933.
- M. L. E. Olyphant, P. Harteck, and Lord Rutherford, "Transmutation Effects Observed with Heavy Hydrogen," Proceedings Royal Society A144, 692 (1934).
- R. B. Roberts, "Investigation of the Deuteron-Deuteron Reaction," Physical Review 51, 810 (1937).

DOCUMENT ROOM

REC. FROM Eng-1

DATE 2-9-50

REC.  NO. REC. \_\_\_\_\_